

How to Make Elastomers Piezoelectric?

Francis Owusu,* Thulasinath Raman Venkatesan, Frank A. Nüesch, Ricardo Martin Negri, and Dorina M. Opris*

Piezoelectrics play a significant role in modern electronics and electric devices. Thermal or mechanical stress on such materials induces a change in polarization generating an electric response, which is the sole effect of why they are so interesting. However, most piezoelectrics are rigid and brittle ceramics and thus difficult to integrate into wearable electronics that comply with human skin or organs. To facilitate their incorporation into stretchable, so-called next generation electronic devices, researchers have focused on developing piezoelectric materials with improved properties. Significant advances are achieved regarding flexibility. However, marrying piezoelectricity and elasticity proved challenging, as elastomers, with their amorphous flexible network structure, cannot keep polarization permanently. Herein, the most recent developments in the field of piezoelectric elastomers are reviewed, and potential future applications in sensors and energy harvesting are discussed.


F. Owusu, T. R. Venkatesan, F. A. Nüesch, D. M. Opris
Laboratory for Functional Polymers
Swiss Federal Laboratories for Materials Science and Technology Empa
Überlandstrasse 129, Dübendorf CH 8600, Switzerland
E-mail: francis.owusu@empa.ch; dorina.opris@empa.ch

F. Owusu, F. A. Nüesch
Institute of Chemical Sciences and Engineering
Ecole Polytechnique Federale de Lausanne (EPFL)
Station 6, Lausanne CH-1015, Switzerland

F. A. Nüesch
Institute of Materials Science and Engineering
Ecole Polytechnique Federale de Lausanne (EPFL)
Station 6, Lausanne CH-1015, Switzerland

R. M. Negri
Institute of Physical Chemistry of Materials
Environment and Energy (INQUIMAE)
University of Buenos Aires
National Council for Scientific and Technical Research (CONICET)
Buenos Aires C1428EGA, Argentina

R. M. Negri
Department of Inorganic
Analytical and Physical Chemistry
School of Exact and Natural Sciences
University of Buenos Aires
Buenos Aires C1428EGA, Argentina

 The ORCID identification number(s) for the author(s) of this article can be found under <https://doi.org/10.1002/admt.202300099>

© 2023 The Authors. Advanced Materials Technologies published by Wiley-VCH GmbH. This is an open access article under the terms of the Creative Commons Attribution-NonCommercial-NoDerivs License, which permits use and distribution in any medium, provided the original work is properly cited, the use is non-commercial and no modifications or adaptations are made.

DOI: 10.1002/admt.202300099

1. Introduction

Electroactive materials exhibit very interesting and useful properties, including piezo-, pyro-, and ferroelectric. They are commonly referred to as “electrets”. Piezoelectricity, primarily discovered in crystalline materials, has found applications in areas ranging from sensors and actuators to energy harvesting.^[1,2] Piezoelectric ceramics and fluorinated polymers have captivated much interest over the last century. Similarly, dielectric elastomers (DEs), a relatively new class of electroactive polymers originally developed for actuator applications in the early 1990s, have extended its portfolio also to include other applications such as energy generators, sensors, etc.^[3,4] Such devices require an external power supply for operation. Due to the variation of polarization, piezoelectrics can generate an electric signal by scavenging thermal and mechanical energy from the surrounding environment and thus can be used as generators and sensors. They, therefore, do not need an external power supply. The possibility of scavenging energy from the human body is particularly attractive, as this may allow powering stretchable biomedical electronic devices.

While piezoelectric ceramics such as lead-zirconate-titanate (PZT) show very good piezoelectric response, they are brittle and, thus, unsuitable for stretchable devices. Piezoelectric polymers must possess molecular dipoles, which have to be polarized to introduce a permanent polarization (at lower temperature). They are either semicrystalline or amorphous. Semicrystalline polymers have small crystalline phase surrounded by amorphous phase. This is the case for poly(vinylidene difluoride) (PVDF), the workhorse piezoelectric polymer and its derivative copolymers. They are flexible and stretchable to a certain extent, but show a lower piezoelectric response than ceramics.^[3,5,6]

In polar amorphous polymers, the dipoles can be polarized above T_g in a strong electric field and the polarization then be locked into a quasi-stable state below T_g . However, such materials are hard, not stretchable, and show a low piezoelectric response. Contrarily, polar DEs are soft and stretchable, offering several advantages over ceramic and semicrystalline polymers to be used in electroactive applications. Despite their molecular dipoles and easy polarization in an electric field, the oriented dipoles randomize after electric field removal and therefore, no permanent polarization can be introduced. This is due to the high mobility of the polymer chains, which favor dipole randomization. Consequently, polar DEs above T_g are not piezoelectric.

Different approaches to stretchable piezoelectric materials have been designed in the literature with a common intention

of intermarrying piezoelectricity and elasticity. Depending on the processing history, piezoelectric elastomers can offer additional freedom in fashioning them into complex device geometries. Such freely shaped devices can be significant in applications ranging from wearable electronics, stretchable wireless sensor networks, soft robotics, and energy harvesting.^[7–13] Regardless of the rise of piezoelectric elastomers in the last decade, there remains a need to close gaps in tailoring suitable materials for optimal and sustainable implementation industrially.^[7,14–17]

There are several reviews on the synthesis and fabrication of piezoelectric materials and their application in wearable electronics, soft robotics, energy harvesting, sensors, actuators, and bio-implantable, among others.^[18–22] Park et al. presented a brief overview of flexible and stretchable piezoelectric nanocomposite generators for realizing self-powered energy systems focusing on development history, power performance, and applications.^[23] Chorsi et al. thoroughly reviewed different piezoelectric biomaterials focusing on operational principles, possible applications in biosensors and bioactuators, as well as their future opportunities and challenges.^[15] Zhou et al. gave an overview of the recent development in new intrinsically stretchable piezoelectric materials and rigid inorganic piezoelectric materials with novel stretchable structures for potential application in sensors and energy harvesters.^[24] Chen et al. discussed recent progress in adopting additive manufacturing for piezoelectric material design, summarizing the advantages of the technology and its technical impact on production.^[14] Another recent review by Vallem et al. briefly summarized the various modes of converting ambient energy sources into electricity using soft and stretchable materials, shedding more light on the harvesting mechanisms and the design strategies to render such devices into soft or stretchable embodiments.^[25] However, here we present a compilation of processing techniques aimed at piezoelectric elastomeric devices. First, we will briefly present the history of piezoelectricity and the underlying fundamental principles from the material perspective. Second, the processing techniques employed in preparing piezoelectric elastomers will be covered, giving typical examples of materials and their inherent properties. To conclude, we will discuss the challenges associated with designing piezoelectric elastomers and point toward the fact that fabricating the best piezoelectric material has to be tailored to a specific application.

2. Brief History and Fundamental Principles of Piezoelectricity

The concept of piezoelectricity revolves around a complex phenomenon that extends across areas of classical physics, electronics, material science, engineering, etc. In connection with the multidisciplinary nature, research publications on this subject are widely scattered, and few books on this topic are compilations of authors' research works. Therefore, piezoelectricity may not necessarily be taught for didactic purposes and can be difficult to understand sometimes. In this section, we will briefly cover the historical milestones of piezoelectricity with a focus on the underlying principles of the phenomenon.

2.1. Historical Milestones

The term piezoelectricity, which Wilhelm Gottlieb Hankel proposed in 1881, combines two Greek words and means “pressure-induced electrostatic charge”. Piezoelectricity is a phenomenon that involves electromechanical interconversion between mechanical stress and electrical polarization.^[26,27] It was discovered in 1880 by Pierre and Jacques Curie. They observed the mechano-electrical transduction effect, also termed direct piezoelectricity, in hemihedral crystals of quartz, tourmaline, zincblende, topaz, boracite, calamine, and Rochelle salt. As a result of the difficulties and lack of knowledge in quantifying the magnitude of this effect, the Curie brothers got stuck in answering only qualitative questions. In 1881, Gabriel Lippmann predicted the existence of the electromechanical transduction effect known as converse piezoelectricity. This was confirmed experimentally by the Curie brothers, who paved the way for quantitative evaluations to reveal the rules governing charge development by pressure.^[3,28]

The early history of piezoelectricity until the scientific community acclaimed the works of the Curie brothers answered interesting questions about how and why the phenomenon was discovered and how the related knowledge was developed. Although scientific discoveries usually have similarities regarding historical patterns, piezoelectricity seems to defy customary trends. The Curie brothers deliberately experimented on this phenomenon, which was not discovered accidentally. The discovery was neither based on an empirical confirmation of established theory nor based on a result of any ‘crisis state’. It was neither an accomplishment based on a new instrument nor an experimental method. However, contingency, theoretical speculations, and derivations based on knowledge of pyroelectric phenomena coupled with experimentation resulted in the discovery of piezoelectricity.^[28,29]

Scientists in the late 19th century enthusiastically embraced the seminal publications of the Curie brothers. Consequently, piezoelectricity was first discovered and investigated in inorganic single-crystal or polycrystalline materials.^[30] The first decade following the discovery was dedicated to understanding the basic properties of the phenomenon with a focus on relations between elastic forces and electric fields. The theory that embraced these properties was successfully formulated based on the pinnacle works of Woldemar Voigt between 1890 and 1894.^[31] Technological applications were not the main concern in the early study of piezoelectricity. Not until the early 1910s when the presence of the phenomenon in quartz was deployed outside the laboratory in sonar to track German submarines during the First World War.^[28,32] The use of quartz was further exploited in the field of frequency control to stabilize oscillators often employed in time-keeping devices, which exceeded that of astronomy based references in stability. However, the avalanche in the electronic applications of piezoelectricity was realized with barium titanate (BaTiO_3), which was demonstrated in 1946 to show forth piezoelectric effect when electrically poled. Phonograph pickups were, as a consequence, the first commercial device made from BaTiO_3 piezoceramics ≈ 1947 .^[1] Following the report of piezoelectricity in BaTiO_3 ceramics, a large array of ceramic materials have been discovered to possess this effect.^[33] For example, PZT discovered in 1954, exhibits outstanding piezoelectric properties. Several other single-crystal materials, such as lithium niobate (LiNbO_3),

lithium tantalate (LiTaO₃), lithium sulfate monohydrate (LSM), ammonium dihydrogen phosphate (ADP), were found to be piezoelectric. Since then, man-made piezoelectric materials have found wide applications in sonar, piezoignition systems, accelerometers, hydrophone, microphones, ultrasonic transducers, frequency-controlled oscillators in watches and radars as well as surface acoustic wave devices employed as major signal processors and detectors in modern telecommunication systems.^[34,35]

Observation of the piezoelectric phenomenon was fortunately not restricted to only ceramic materials. Eiichi Fukada and other scientists, in the 1950s and 1960s, pioneered the field of piezoelectricity in wood, collagenous tissues, and bio- and synthetic polymers.^[36–42] Particularly interesting to the wider scientific community was the discovery of the piezoelectric effect in PVDF by Heiji Kawai in 1969.^[43] Further investigations in the 1970s were carried out on copolymers of PVDF with vinyl fluoride, trifluoroethylene, and tetrafluoroethylene by several scientists.^[3,44,45] The effects in these synthetic polymers were at least an order of magnitude higher than previously observed in other biomaterials and represent state-of-the-art piezoelectric polymers.^[46,47] In later years, piezoelectricity has been investigated in several other polymer-based materials ranging from biopolymers, amorphous polar polymers, solid and cellular polymer electrets, ceramic–polymer hybrids, electret elastomers, etc.^[26,35,48–65] For instance, in 2001, the VTT Technical Research Centre of Finland reported on a film made from polypropylene with a cellular structure that exhibited piezoelectric sensitivity of 200 pC N^{−1}.^[66] Thus far, the thermal stability of the piezoelectric response, which is only guaranteed up to 60 °C, has been the major limitation for many applications. In the same year, Gerhard-Multhaupt and co-workers observed in corona-charged sandwich films of porous amorphous Teflon a strong piezoelectric effect up to 600 pC N^{−1}, which was thermally stable up to 120 °C.^[67] Additionally, a Swiss company named Algra group introduced printable piezoelectric composite materials with sensitivity up to 1000 pC N^{−1} in device configurations and are commercially employed in touch switches and keyboards.^[3] Details of these materials remain a company secret. In summary, piezoelectricity has received enormous research attention over the years and is progressively drifting the search toward sustainability with a keen interest in flexible and stretchable polymeric materials.

2.2. Origin of the Piezoelectric Effect in Different Materials and Related Equations

Theoretically, piezoelectricity can be understood as an electromechanical coupling between mechanical and electrical states. The existence of a non-centrosymmetric structure is a prerequisite for piezoelectricity. In the case of nonferroelectric crystals such as quartz, the phenomenon can be explained with a simple molecular model, as shown in **Figure 1**.^[68] Before applying mechanical stress, the poled material does not possess any static surface charges and is electrically neutral, as indicated in **Figure 1a**. When pressure is exerted, the internal reticular structure is deformed, which causes the opposite charge centers in the molecule to separate and eventually leads to the generation of a small dipole, as shown in **Figure 1b**. An ideal situation for a material containing such molecules is that the opposite-facing poles

of each molecule are mutually canceled, and fixed charges appear on the surface of the bulk material, as illustrated in **Figure 1c**. That is to say, the application of mechanical stress results not only in a strain response but also in an electrical polarization. In the case of polar ferroelectric materials such as PZT and PVDF, spontaneous polarization exists in the material below their respective Curie transition temperature. Hence, after poling, the dipoles can be oriented in the direction of the applied electric field, resulting in static charges induced on the electrode of the sample, as shown in **Figure 1d**. The piezoelectricity in these materials arises from intrinsic or extrinsic effects or a combination of both. Intrinsic effects arise from the displacement of positive and negative charges (change in dipole moment) on the application of external stress, as in the case of nonferroelectric materials or due to a change in dipole density (**Figure 1e**). In PVDF, the main contribution to the piezoelectric effect comes from the change in dipole density.^[3] The extrinsic effect is generally described as a result of displacement of non-180° domain walls, which is dominating in piezoelectric ceramics such as BaTiO₃ and PZT.^[69] Overall, applying external stimuli increases the induced charges on the electrode due to intrinsic and extrinsic piezoelectric effects in the material leading to a charge flow as shown in **Figure 1c,e**.

In principle, the piezoelectric effect is a reversible process. Thus, the direct effect displaces charges in response to applied mechanical stress. The converse effect is the mechanical strain when an external electric field is applied, as schematically illustrated in **Figure 2**. Thermodynamic principles have been used to model these phenomena to interpret or quantify observed experimental results, as referenced in the IEEE Standards on Piezoelectricity, even though other models were developed based on microscopic theories with appreciable clarifications.^[72,73]

Linear approximations describe the piezoelectric effect and are valid in small mechanical deformations and electric fields. However, the phenomena may exhibit nonlinearity above certain thresholds upon applying an electric field or mechanical stress. This review focuses on the linear theory of piezoelectricity in which the elastic, piezoelectric, and dielectric coefficients are treated as constants independent of the magnitude and frequency of the applied mechanical stress and electric field as clearly described in the scope of the IEEE standards.^[72]

Following energy exchange and thermodynamic considerations, appropriate constitutive equations could be formulated as follows

$$\begin{bmatrix} S \\ D \end{bmatrix} = \begin{bmatrix} s^E & d^T \\ d & \epsilon^T \end{bmatrix} \begin{bmatrix} T \\ E \end{bmatrix} \quad (1)$$

$$\text{Direct piezoelectric effect } D = \epsilon^T E + d^T T \quad (1a)$$

$$\text{Converse piezoelectric effect } S = d^T E + s^E T \quad (1b)$$

where D and E denote the dielectric displacement and electric field components; S and T refer to the mechanical strain and stress components; s , ϵ , and d represent the elastic compliance, the dielectric permittivity, and the piezoelectric coefficient, respectively. The superscripts E and T indicate that the respective quantities are measured at a constant electric field and constant

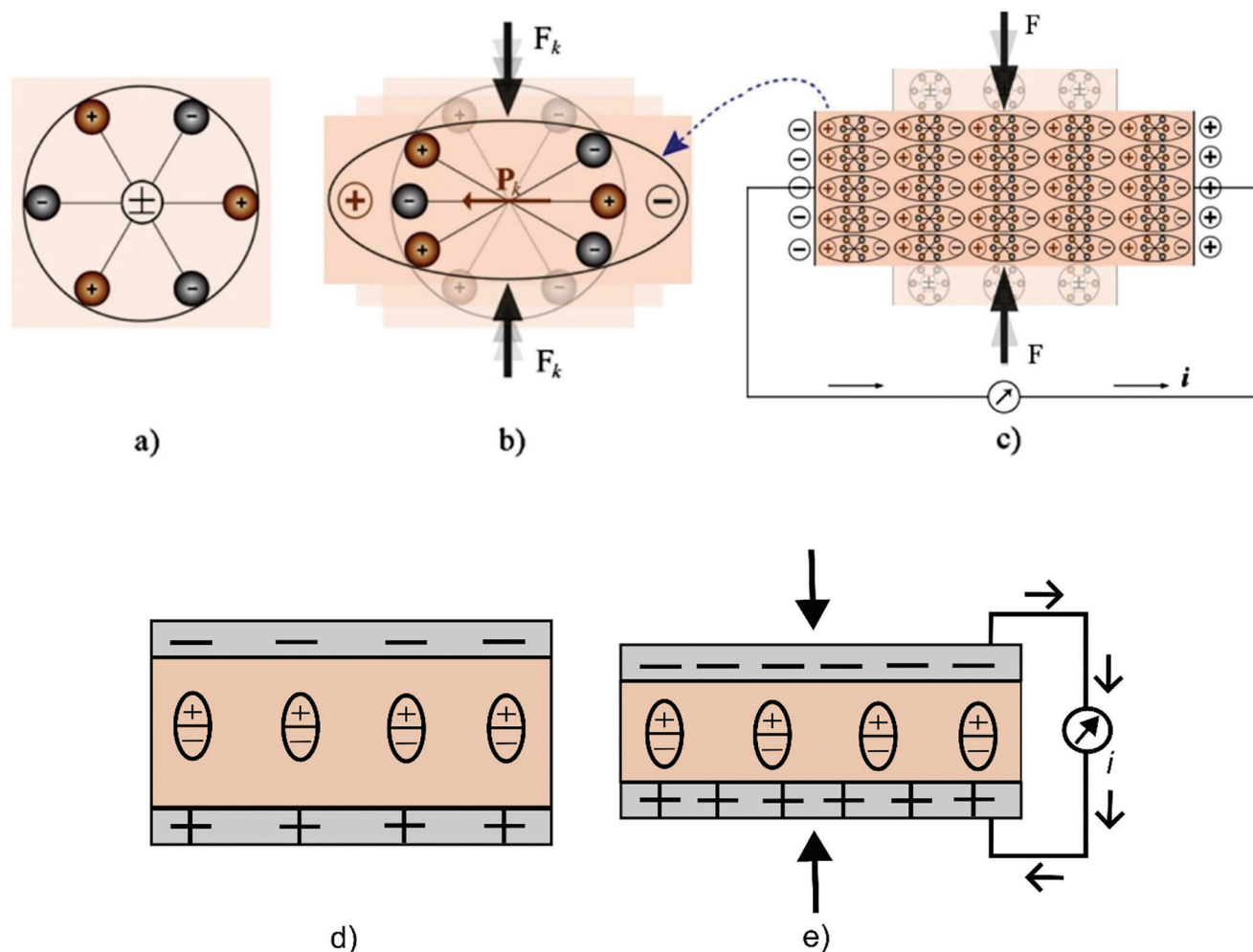


Figure 1. Piezoelectric effect explained with a simple model in nonferroelectric and ferroelectric materials. a) An unperturbed molecule with no piezoelectric polarization (though prior electric polarization may exist). b) The molecule subjected to an external force (F_k), resulting in polarization (P_k) as indicated. c) The polarizing effect on the surface when a piezoelectric material is subjected to an external force. Reproduced with permission. Adapted with permission.^[70] Copyright 2013, Springer. d) Poled ferroelectric material containing oriented permanent dipoles inducing static charges on the metal electrode. e) Change in dipole density on the application of external stress resulting in charge flow between electrodes.

mechanical stress, respectively, and superscript t stands for the transpose. It is equally possible to develop second partial derivatives of the Gibbs free energies for the four different configurations of natural variables ((T,D) , (T,E) , (S,D) , and (S,E)) and obtain four matrix equations that describe the same piezoelectric system, but based on different boundary conditions. These equations can easily be found in the literature.^[74]

Numerous mechanistic and phenomenological models are proposed in the literature to explain the philosophy behind the origination of the piezoelectric effect in different kinds of material systems.^[1,24,29,46,49,52,66,68,71,73,75–90] However, a more simplified and semiquantitative model (termed as a charge-spring model) proposed by Gerhard has specifically been useful in the design of soft, flexible, and stretchable piezoelectric materials as well as predicting their electromechanical behaviors.^[26,91] This model generally considers a piezoelectric material as a two-phase system with a dipole phase and a matrix phase, which is elastically nonaffine. The dipole phase usually comprises nano-, micro-,

or macroscale units such as ionic charges of opposite polarity in the lattice of inorganic solid, polar molecules, ionic crystalline particles, polar crystallites in a semicrystalline polymer, polar particles with opposite charges on their opposing faces, cavities with internal surface charges of one or both polarities, etc. The matrix phase can be the boundary layers between or around ionic charges, the polymer matrix of a composite, the amorphous phase of a semicrystalline polymer, the cell walls of a polymer foam, etc. The length scales of the two phases and their deformations are different in these materials. The dimension of the two phases, particularly the lengths of the respective springs in the model, may range from a few nanometers in crystalline materials to micrometers or millimeters in semicrystalline polymers or various composites.

This concept can be represented by the arrangement of charges and springs (Figure 3).

In an ideal case, electric polarization P in a material of volume V can be represented mathematically by the vector sum of

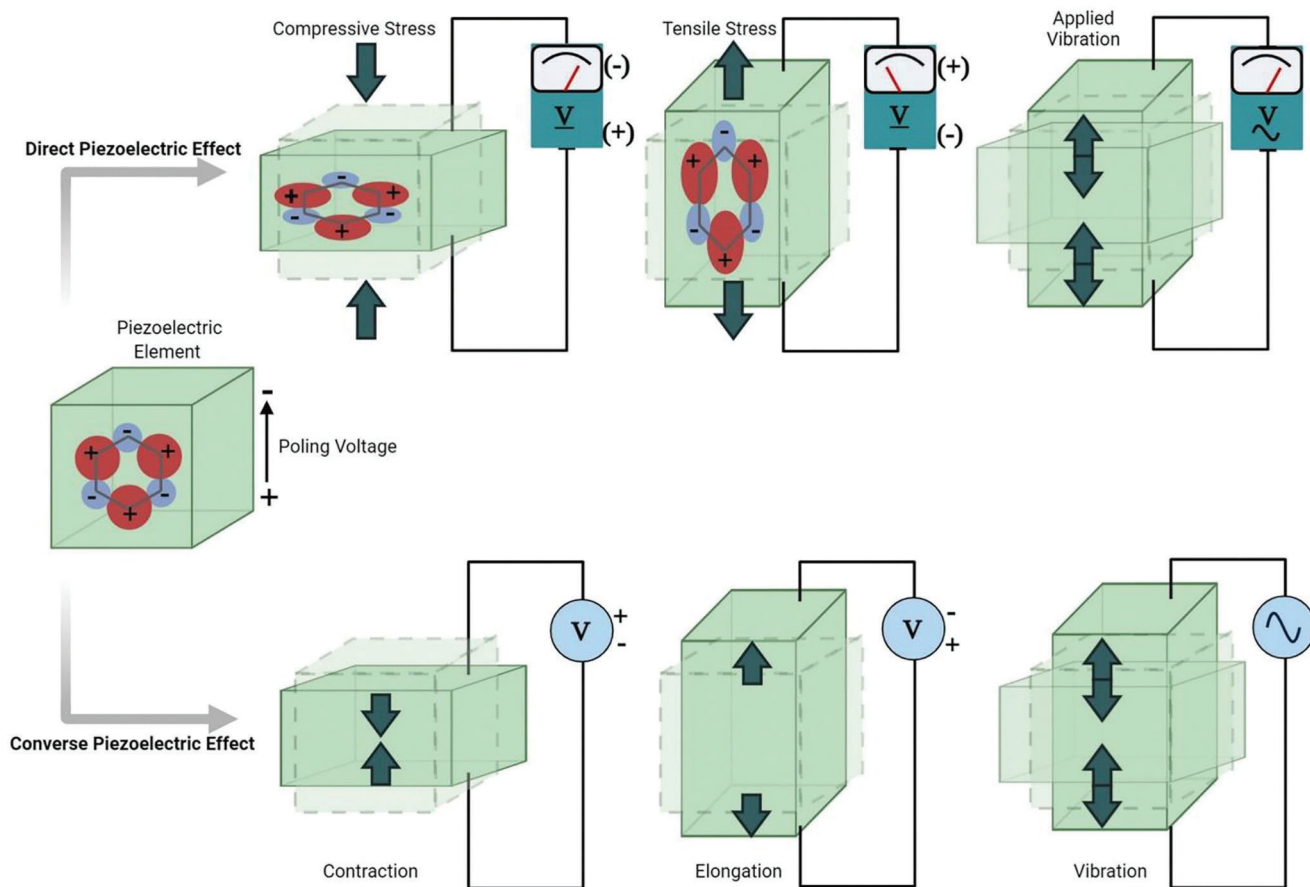


Figure 2. The piezoelectric effect. The direct piezoelectric effect generates an electric voltage in response to a mechanical force, whereas the converse piezoelectric effect produces mechanical stimulation in response to an electric voltage. Reproduced with permission.^[71] Copyright 2021, Mary Ann Liebert, Inc.

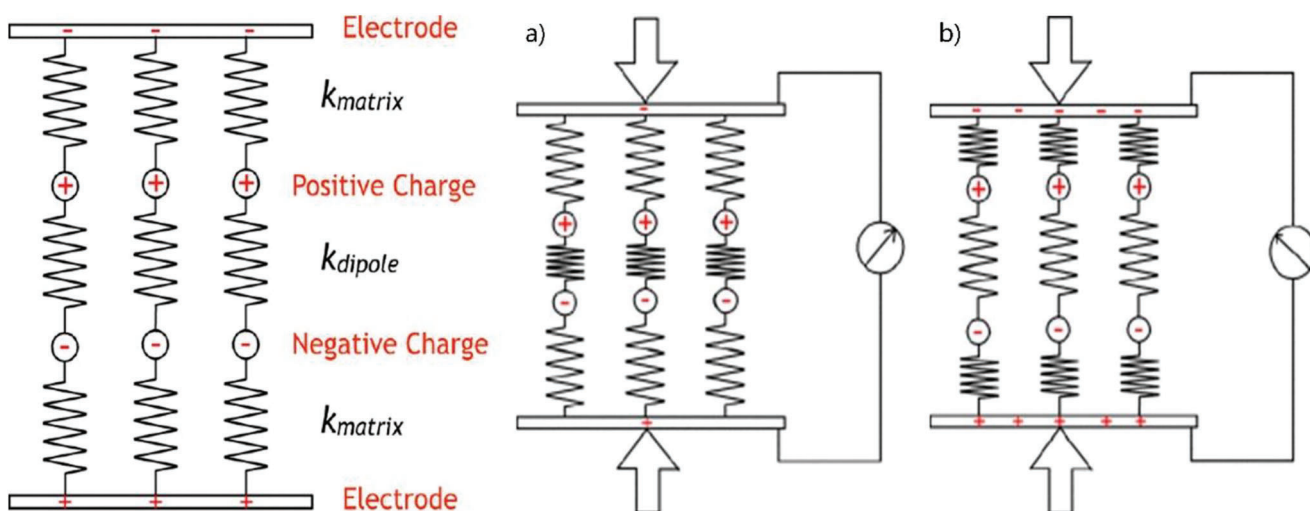


Figure 3. Charge-spring model for an elastically heterogeneous material with a dipole phase, a matrix phase, and interface charges between them. a) Nonaffine deformation $k_{matrix} \gg k_{dipole}$ leads to a dipole moment change (so-called primary piezoelectricity). b) Nonaffine deformation with $k_{matrix} \ll k_{dipole}$ leads to a dipole density change (so-called secondary piezoelectricity). Reproduced with permission.^[91] Copyright 2014, SPIE.

its dipole moments μ as

$$\vec{P} = \frac{1}{V} \sum_{i=1}^N \vec{\mu}_i \quad (2)$$

By definition, dipole moment μ is the product of charge magnitude q_i and the distance l_i between the centers of the opposite charges, which can be expressed as $\vec{\mu}_i = q_i \vec{l}_i$. Following this expression, Equation (2) can be rewritten as

$$\vec{P} = \frac{1}{V} \sum_{i=1}^N q_i \vec{l}_i \quad (3)$$

Applying a mechanical stress component T to a poled material gives a corresponding linear electrical response called direct piezoelectricity, which is described by the d coefficient. Considering all relevant definitions, the d coefficient can be expressed as the sum of local linear changes in the dipole moments, which has been termed as dipole moment effect or “primary piezoelectricity” and the dipole density, also termed as matrix effect or “secondary piezoelectricity”. These two contributing terms are illustrated in Figure 3a,b, and can be mathematically expressed in the following response equation

$$\frac{\partial \vec{P}}{\partial T} = -\frac{1}{V^2} \frac{\partial V}{\partial T} \sum_{i=1}^N q_i \vec{l}_i + \frac{1}{V} \sum_{i=1}^N q_i \left(\frac{\partial \vec{l}_i}{\partial T} \right) \quad (4)$$

In a special case of a thin film material system subjected to compression in the thickness direction, Equation (4) can further be simplified to achieve an approximated relation that considers only the unified thicknesses of the respective phases t , the bipolar interfacial charge density σ (the overall polarization P_3) and the respective Young's moduli of the dipole (Y_D), and the matrix (Y_M) phases

$$d_{33} \approx \frac{\partial P_3}{\partial T_{33}} \approx -\frac{\sigma}{t} \frac{l_D}{Y_M} + \frac{\sigma}{t} \frac{l_D}{Y_D} \approx -\frac{P_3}{Y_M} + \frac{P_3}{Y_D} \quad (5)$$

Equation (5) clearly shows that the matrix and dipole phases should have different elastic moduli, otherwise, no piezoelectricity is observed. For very stiff matrices with an elastic modulus significantly higher than the dipoles, the change in polarization responsible for the piezoelectric response is due to the reduction of polarization as the charges are squeezed together. When the elastic modulus of the dipoles is higher than the matrix, the polarization in the material increases when the material is pressed, as the matrix will deform. Thus, to achieve materials with a high piezoelectric response, the material's polarization should be as high as possible and the elastic moduli of the dipoles and matrix should be significantly different. The validity of the charge-spring model was confirmed experimentally for both materials. Additionally, the piezoelectric response could be predicted by the product of the remanent polarization in the poled material and its overall elastic modulus. For further understanding, the reader is referred to literature.^[26,30,91,92]

3. Strategies for Piezoelectric Elastomers

This section will emphasize strategies developed over the years to achieve piezoelectric elastomer materials to meet precisely advanced technological application requirements. As elastomers consist of cross-linked highly disordered polymer chains in permanent motion, a permanent polarization cannot be introduced above T_g . Therefore, polarizable fillers have been used in elastic matrices. To achieve elastic composites with a high piezoelectric response, the amount of filler should be as high as possible.^[93] However, high filler amount negatively affect the mechanical properties of the composite. Therefore, compatibilization of the filler with the matrix should be done. Filler's surface can be modified by adding surfactants or by chemical modification with silane reagents. Among the best reagents for this purpose is hexamethyldisilazane, which can efficiently bind to any surface, changing it hydrophobic.^[94,95] If such treatment is insufficient, other silane reagents that allow grafting from or grafting to suitable compatibilizer can be used.^[95] A strong connection between the matrix and filler may allow for improved mechanical properties and a more reliable piezoelectric response. A poor connection between the filler and the matrix may result in void inclusion and a more complex interface where other processes, such as contact electrification, can influence the piezoelectric response.^[96]

As a matrix, any elastomer such as polyurethane, natural rubber, chloroprene, poly(acrylonitrile butadiene) rubber, and polydimethylsiloxane (PDMS) can be used. However, the most explored one is PDMS. This is likely due to the easy processability of thin films and the availability of different formulations with different cross-linking possibilities. Additionally, PDMS elastomers are rather easily developed to suit any application. Furthermore, their mechanical properties can be easily tuned by the cross-linking density and, thus, the length of the segments between the cross-linking points.^[97,98] As predicted by the charge-spring model, the elastic moduli of the matrix and filler should be different to achieve materials with a large piezoelectric response. Therefore, a soft matrix would be attractive. Unfortunately, soft matrices tend to have a low dielectric breakdown field; therefore, a compromise between different requirements and properties must be found. Additionally, common elastomers have a lower dielectric permittivity at room temperature (generally considered as application temperature) than piezoelectric ceramics or fluorine-based polymers (PVDF and its co- and terpolymers), which are commonly used as sensors and energy harvesters. Since higher permittivity is desired in these applications, more efforts have been taken to increase the permittivity of elastomers by incorporating polar groups into the polymer.^[99] The polar groups, however, increase the T_g of the elastomer. From the application's point of view, it is preferred to have elastomers with a T_g significantly lower than room temperature.

The other major parameter affecting the performance of elastomers as sensors and harvesters is their ionic conductivity. Above the T_g of the elastomer, the polymer chains are mobile, which facilitates ion-related motions resulting in a steep increase in dielectric losses. For dielectric applications, this increase in conductivity is detrimental as it will result in increased dielectric losses, aging effects, etc. Hence, the elastomer used should have low ionic conductivity.

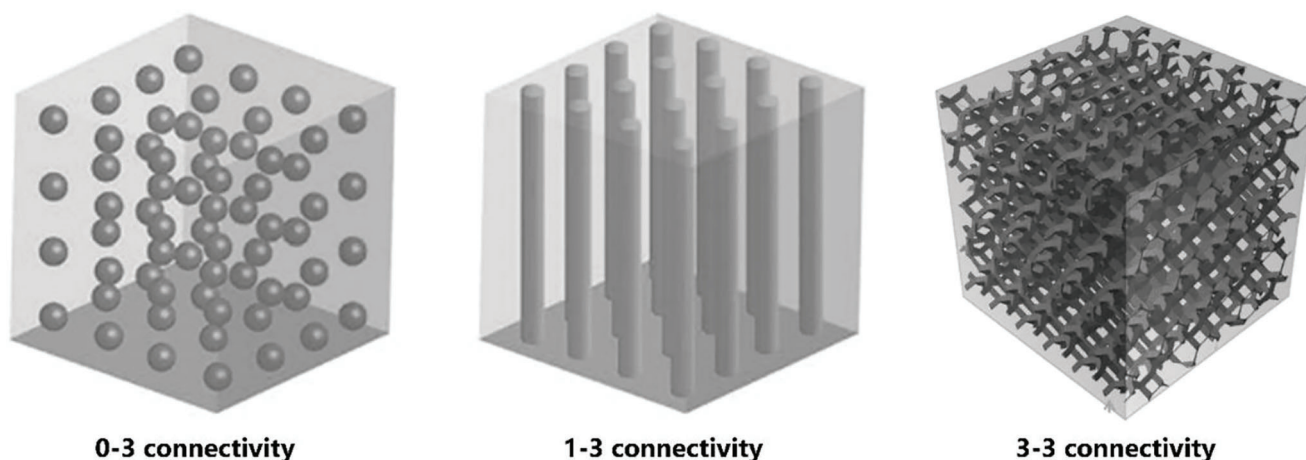


Figure 4. Schematic illustration of ceramic–polymer composite connectivity patterns. Reproduced with permission.^[11] Copyright 2018, Wiley–VCH GmbH; Reproduced with permission.^[106] Copyright 2018, Royal Society of Chemistry.

In the following subchapters, different strategies used for the synthesis of piezoelectric elastomers will be described.

3.1. Ceramic–Polymer Compositing

To quickly remind the readers about bulk piezoelectric ceramics, it should be mentioned that though they undoubtedly exhibit high piezoelectric performance, they are too brittle to be integrated into flexible and stretchable electronics. Therefore tailoring heterogeneous composite with locally tuned elastic properties would extend the lifetime of functional devices employed at mechanically incompatible interfaces and create materials for application in flexible and stretchable electronics. Processing ceramic–polymer composites involves mixing melt polymers or polymeric solutions with ceramic particles. In preparing such diphasic hybrid materials, it is important to consider the properties of the individual phases, their relative amounts, and the preferable manner of interconnection.^[100] The concept of connectivity implies the number of dimensions a component phase in the composite can be self-connected. A diphasic composite system can have at least ten predictable connectivity patterns, ranging from 0–0, where neither phase is self-connected, to 3–3, where each phase is self-connected in three dimensions.^[101–103] The first digit denotes the connectivity of the filler particles, while the second represents the host matrix. Typically in a piezoelectric elastomer material made from ceramic filler and a passive polymer matrix, the success of such a hybrid system can be traced to a well-designed connectivity of each phase making up the composite. The connectivity patterns help control the effectiveness of stress transfer in the hybrid material and enhance the anisotropy of property coefficients. Thus, the number of dimensions in which the piezoelectric ceramic filler particles and the elastomeric polymer matrix are self-connected influences the piezoelectric coefficient and the elastic modulus of the resultant material.^[102,104,105]

A typical traditional method for processing such hybrid materials involves random dispersion of the ceramic filler particles in a continuous polymeric phase, which mostly results in a 0–3

connectivity pattern. Achieving good connectivity in the ceramic phase by such an easy technique usually requires increasing the volume fraction above the percolation threshold, eventually compromising the resulting composite's mechanical flexibility and elasticity. In 0–3 composites, the active filler phase has zero connectivity, while the inactive matrix phase has 3D connectivity. The 1–3 case refers to active filler connectivity in one dimension, while the matrix phase is continuous in all three dimensions. The 3–3 denotes each phase is self-connected in all three dimensions. We will, in this context, describe some processing techniques that have been deployed practically to attain 0–3, 1–3, and 3–3 connectivity patterns in piezoelectric ceramic–polymer composites, as illustrated in **Figure 4**.

3.1.1. Piezoelectric Composites with 0–3 Connectivity

The 0–3 type piezoelectric filler composites have the advantages of easy synthesis and manufacturing in different shapes and film thicknesses with large areas. Various fillers and matrices were investigated.^[107,108] Because of the favorable combination of piezoelectric and elastic properties, PZT and BaTiO₃ fillers and PDMS matrix were the most explored. Already in 1959, Lutsch dispersed BaTiO₃ particles in an organic resin and poled it in a strong electric field above the Curie temperature of the filler. He found a strong influence of the particle size on the piezoelectric response, e.g., the smaller the filler size, the lower the response.^[109] Later, Qian et al. developed BaTiO₃ composites in a silicone matrix. A piezodevice with a size of 5 × 6 cm² gave peak-to-peak values of a voltage of 38 V and a current of 0.8 μA and could charge a capacitor of 1 μF to 14 V in 800 s.^[110]

Composites of PZT particles with different sizes of 30, 50, and 80 μm in a rubber matrix poled at 50 kV cm^{−1} gave a d_{33} of 29, 36, and 46 pC N^{−1} and a d_{31} of −8, −11, and −14 pC N^{−1}, respectively.^[111] Banno investigated composites of PZT and PbTiO₃ in chloroprene rubber and reported a piezoelectric coefficient d_{31} of about −5 pC N^{−1}.^[112,113] Changing the ratio between the PZT/PbTiO₃ did not lead to a significant difference in the d_{31} response. Choudhry et al. dispersed

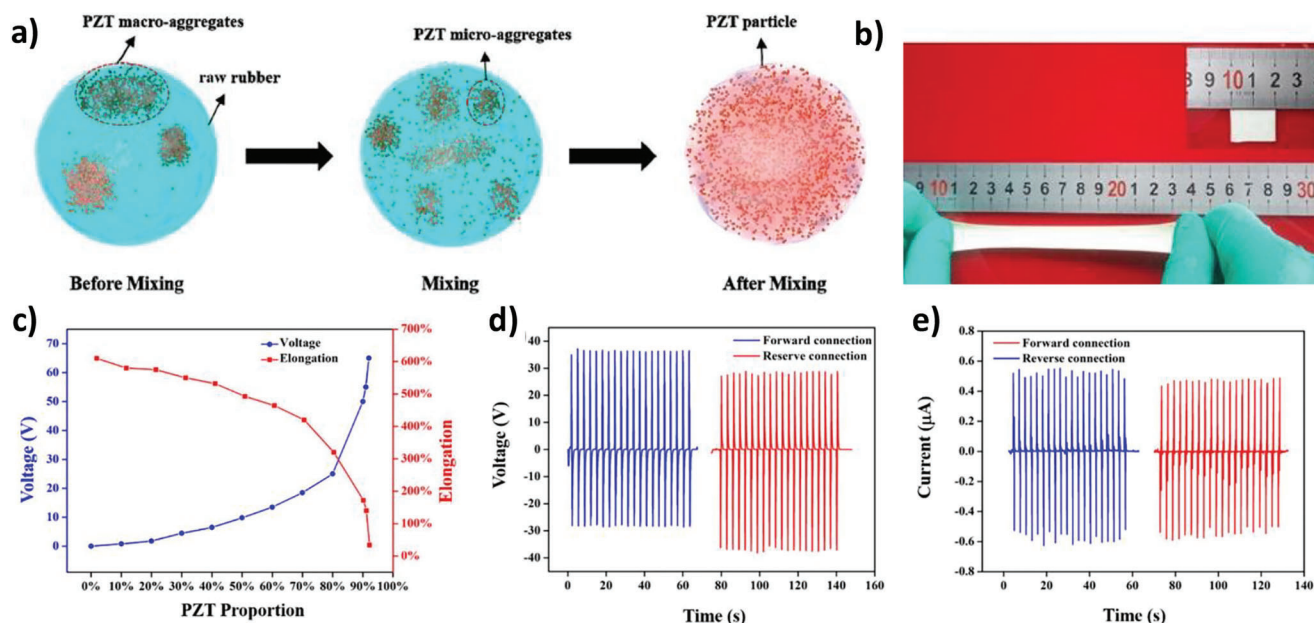


Figure 5. PZT-based stretchable piezoelectric nanogenerator (HSPG). a) Fabrication process, b) the piezoelectric composite is stretched to 575%. c) The maximum output voltages and elongations at break of HSPGs with different PZT proportions. The measured d) output voltage and e) currents of the HSPG with forward and reverse connection. Reproduced with permission.^[121] Copyright 2019, American Chemical Society.

different piezoelectric nanoparticles (BaTiO₃, ZnO, and PZT) in a PDMS matrix and found that the PZT-based composites are superior, giving an open-circuit voltage (≈ 27 V), short-circuit current (429.23 μ A), and power density (402 mW m⁻²) under real-time human walking.^[114] 85 vol% of lead magnesium-niobate (PMN) in poly(acrylonitrile butadiene) rubber poled at 7–8 kV mm⁻¹ and 80 °C showed a $d_{33} = 33$ pC N⁻¹.^[115] Later, a composite film of lead magnesium niobate-lead titanate (PMNPT) in an elastic matrix sandwich between silver nanowires stretchable electrodes and poled at 50 kV cm⁻¹ gave an output of 4 V and 500 nA and exhibited no significant degradation during about 15 000 stretching–relaxation cycles.^[116] A piezoelectric device (5 cm \times 4 cm) consisting of PZT (65 vol%) in a silicone elastomer matrix, when strained 50% at 6.4 cm s⁻¹ strain rate and a frequency of 0.7 Hz, generated an output voltage of 20 V, a current of 0.55 μ A, and a power density of 3.93 μ W cm⁻³.^[117] Liu et al. made a ternary composite of graphene and PZT in silicone. The PZT:PDMS composite and the optimized ternary-based piezoelectric composite with 0.33% graphene exhibit slightly smaller output voltage but much greater short-circuit current density of 13.23 μ A cm⁻² under foot stepping. The output power of 32 nW (59 mV and 553 nA) and 1.9 nW were measured for the 0.33% graphene/PZT/PDMS composite and the PZT/PDMS, respectively.^[118] An elastic PZT composite in a hydrogenated styrene–butadiene block copolymer, which can be stretched to $\approx 950\%$, gave a maximum output current density of 9.704 mA m⁻² and an open-circuit voltage of ≈ 100 V. The device can power 40 green light-emitting diodes (LEDs) and charge a 10 μ F capacitor from ≈ 0 to 6 V in ≈ 500 s.^[119]

Quinsaat et al. developed piezoelectric elastic polydimethylsiloxane-based composites with a volume content of 37–72 vol% PZT filler (particle sizes of 2 and 20 μ m) and

achieved piezoelectric responses of d_{33} and d_{31} of 2.7–40 and 16–48 pC N⁻¹, respectively.^[120] A composite of 38 vol% PZT filler (20 μ m particle size) in a commercial PDMS exhibited long-term mechanical stretchability and a $d_{33} = 3.6$ pC N⁻¹ and $d_{31} = 30$ pC N⁻¹, respectively. The commercial availability of filler and metrics facilitates the implementation of this material in applications.

The piezoelectric response of 0–3 composites increases with the amount of piezoelectric filler used. Unfortunately, this has a detrimental effect on mechanical properties. To circumvent this problem, Niu et al. used agglomerated PMNPT particles and increased the amount of active filler to 92 wt% while the composites could still be stretched by 30% (Figure 5). The generators produced a power density of about 81.25 μ W cm⁻³. The best material showed a peak-to-peak voltage of 50 V and could charge a capacitor of 10 μ F up to ≈ 10 V in 20 min.^[121]

3.1.2. Piezoelectric Composites with 1–3 Connectivity

Several strategies have been used to synthesize composites with 1–3 connectivity, however, dielectrophoresis is the most explored. It was first reported in 1949 by Winslow when describing a phenomenon whose origin is electrically induced by the alignment of small particles in liquid fluid suspensions.^[122] The technique has since been employed as a relevant step in processing piezoelectric elastomer composites with ceramic particles as the filler phase and elastomeric polymers as the matrix phase. In principle, such hybrid materials are subjected to an AC electric field before cross-linking, which evokes a translational force causing the particles to reorient with respect to the electric field.^[123] The nonuniform electric field, as a result, induces space charge

separation on each suspended particle which then generates a dipole. The induced dipoles from the displacement of double layer and/or space charges at the fluid–particle interface then associate with each other via electrostatic dipolar–dipolar interactions. Eventually, the resultant translational motion causes rotation and axial displacements on the suspended particles leading to fibrils of chain-like arrangements, called dielectrophoresis or electrorheological effect.^[124,125] A schematic illustration of this processing technique can be found in **Figure 6**. The advantage of this technique over the traditional method is that a relatively low volume fraction of filler particles can be used to achieve quasi 1–3 connectivity patterns in the resulting composite materials. Additionally, effective stress transfer can be attained in the structured particle phase resulting in excellent piezoelectric properties while preserving the composite material's elastic integrity.

For instance, Gao et al. recently adopted this unidirectional particle alignment engineering technique to fabricate a flexible piezoelectric touch sensor and wearable keyboard with outstanding sensitivity and extraordinary mechanical stability.^[104,105] The sensing element, which was a diphasic composite prepared from 8 vol% of $(\text{Ba}_{0.85}\text{Ca}_{0.15})(\text{Ti}_{0.90}\text{Zr}_{0.10})\text{O}_3$ (BCZT) particles in a PDMS matrix, gave an impressive open-circuit voltage of 28.8 V and a piezoelectric voltage coefficient (g_{33}) of 0.10 V m N⁻¹. By optimizing the poling conditions of this same material composition, the scientists reported an outstanding g_{33} value of 0.60 V m N⁻¹ attributed to synergistic enhancement in the stress-transfer capability of the aligned active particles in the composite material.^[105] Another study by Stuber et al. presented the design of a quasi 1–3 connectivity pattern of potassium sodium lithium niobate (KLN) ceramic fibers in a flexible PDMS matrix by dielectrophoresis.^[102] The energy harvesting performance of the structured composite materials was determined by the product of piezoelectric coefficients, $d_{33} \cdot g_{33}$, which is a measure of the energy density per unit volume that can be harvested. However, these hybrid materials exhibited piezoelectric properties, which are dependent on the aspect ratio of filler particles, their interconnectivity after aligning in the PDMS matrix, and poling efficiency.

Thus, the higher the aspect ratio of the filler fibers used, the shorter the interparticle distance becomes when electrically aligned and the higher the electromechanical coupling. The measured figure of merit, $d_{33} \cdot g_{33}$, was 18 pm³ J⁻¹, reported to be comparable to that of state-of-the-art ceramic PZT. Pseudo-1-3 piezoelectric PZT/polymer composites in different polymeric matrices (silicone gel, silicone rubber, urethane rubber, and poly(methyl methacrylate)) and poled at the different electric fields have also been reported. An increase in the piezoelectric response with the poling field and reducing the elastic modulus of the matrix were demonstrated.^[126]

Another less explored possibility of achieving composites with 1–3 connectivity is making ribbons and pillars of piezoelectric filler on a substrate which are then transferred to an elastic matrix. For instance, crystalline piezoelectric nanoribbon ribbons of PZT on a host substrate were transferred onto PDMS. They showed among the highest electromechanical energy conversion with a transverse piezoelectric constant, $d_{31} = 49$ pm V⁻¹, which could be increased to an even higher value of $d_{31} = 79$ pm V⁻¹ when the structure was poled at ≈ 100 kV cm⁻¹ for 14 h (**Figure 7a–d**).^[127]

To overcome the mechanical incompatibility between inorganic piezoelectrics and elastomeric substrates, PZT was shaped as wavy ribbons (5–10 μm wide and 250–500 nm thick) before transferring to a stretched PDMS film (**Figure 7e**).^[128] Finally, releasing the prestrain in the PDMS led to periodic de-adhesion and buckling of PZT ribbons. A current density of 2.5 $\mu\text{A mm}^{-2}$ was calculated, comparable to the current density measured in PZT nanowire-based devices.

3.1.3. Piezoelectric Composites with 3–3 Connectivity

In 3–3 composites, the piezoelectric filler and the matrix have 3D connectivity. Their syntheses involve two major steps, as illustrated in **Figure 8**. The first step is fabricating cellular ceramic struts with tailored microstructure containing a high porosity (typically above 70 vol%). Methods employed to produce such macroporous ceramics with 3D arrangements include, but are not limited to, replication of porous polymer templates, sacrificial template technique, and direct foaming of a liquid slurry. Detailed descriptions of methods regarding the versatility and ease of fabrication and the influence on the microstructure and mechanical strength of the macroporous ceramics can be found in the literature.^[129–131] The final step involves infiltrating the macroporous interconnected structure with an elastomeric polymer solution and curing it into cross-linked networks.

For instance, Rittenmyer et al. mixed plastic spheres with PZT powder in an organic binder and sintered the mixture to give a ceramic skeleton, which was backfilled with PDMS and poled after curing. Composites containing 50% PZT showed a piezoelectric d_{33} response of about 250 pC N⁻¹.^[132] Hikita et al. showed that the voltage output coefficient of the porous PZT increased with increasing volume fraction of porosity. A high voltage coefficient of 100×10^{-3} V m N⁻¹ was obtained in samples with a volume fraction porosity of 0.6 and thus showed almost the same piezoelectric response as the starting porous PZT.^[133] Varaprasad et al. prepared a porous La-doped PZT 3D structure and infiltrated it with silicone using poly(methyl methacrylate) particles glued by polyvinyl alcohol as a sacrificial template. Best materials had a 50 wt% filler and it was poled at 100 °C and 25 kV cm⁻¹. A d_{33} coefficient of 90 pC N⁻¹ and a piezoelectric voltage coefficient g_{33} of 110×10^{-3} V m N⁻¹ were reported.^[134] Li et al. first made a porous PZT structure via freeze drying and calcination followed by impregnation with PDMS to give a 3–3 piezoelectric composite with a piezoelectric constant $d_{33} \approx 146$ pC N⁻¹, which is almost ten times higher than the conventional 0–3 piezoelectric composite.^[135] Wang and co-workers designed energy harvesters based on 3–3 connectivity patterned composites prepared from ceramic skeletons infiltrated with PDMS.^[106,136,137] The piezoceramic 3D interconnected architectures were prepared using polyurethane (PU) foam and biofibril cellulose as templates. Thus, a sol–gel or slurry of the piezoceramic phase is either dip-coated on the PU foam or freeze-casted in a blend with cellulose solution. Depending on the templating approach, the resulting wet mold is dried using an oven or a freeze-dryer. Afterward, the dried sample is calcined at an elevated temperature to burn out the sacrificial template. Finally, a solution of PDMS is infiltrated into the macroporous ceramic skeleton via vacuum suction and cured. A model based on Fourier spectral iterative

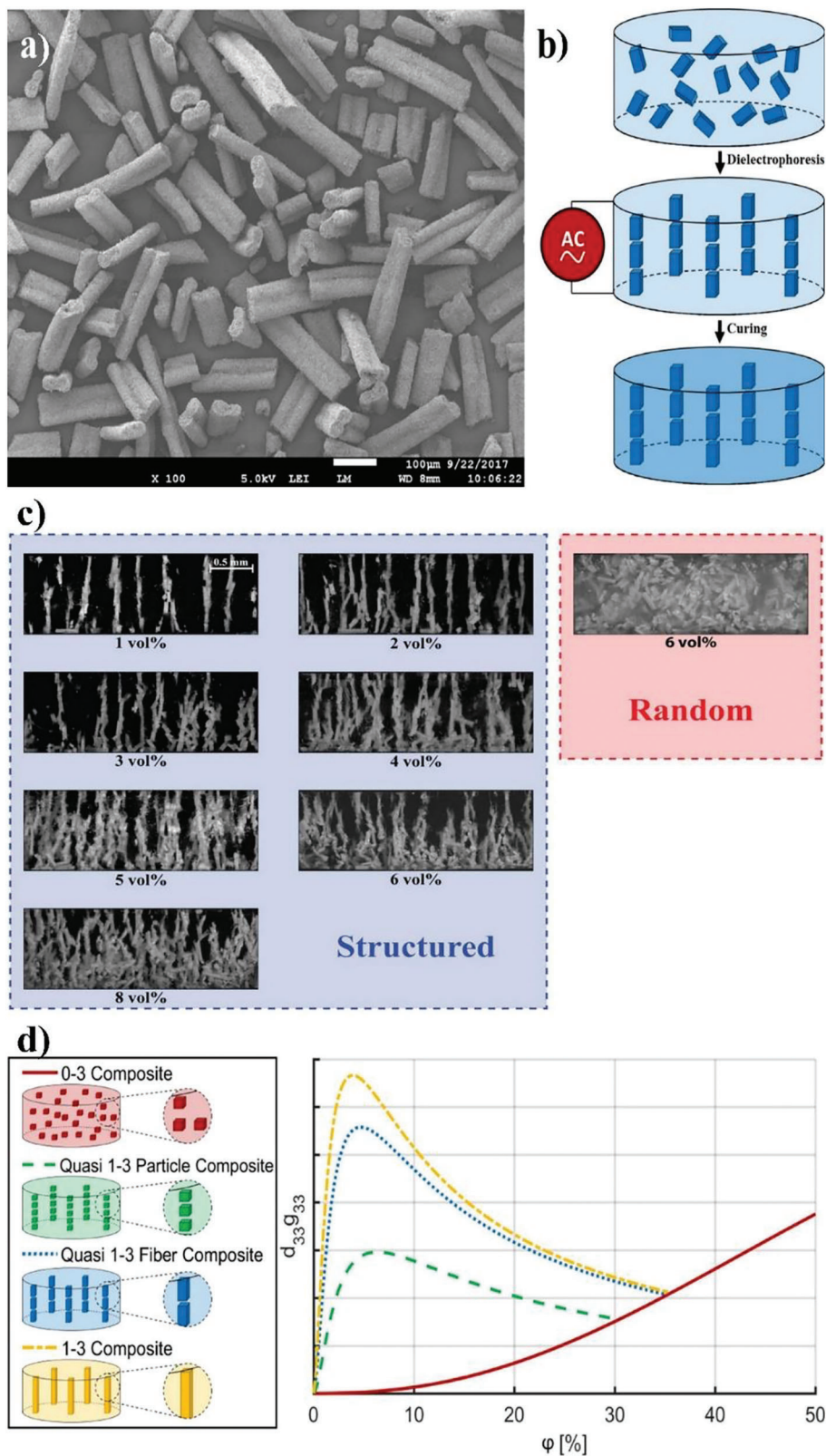


Figure 6. Schematic representation of dielectrophoresis process. a) SEM image of KNLN fibers. b) Typical alignment mechanism of piezoelectric particles. c) Microstructure of dielectrophoretically aligned KNLN fibers in a PDMS matrix. d) Connectivity schemes of ceramic-polymer composite materials and corresponding arbitrary illustration of the energy harvesting figure of merit, $d_{33} \cdot g_{33}$ as a function of volume fraction, ϕ , of piezoelectric filler. Reproduced with permission.^[102] Copyright 2019, Wiley-VCH GmbH.

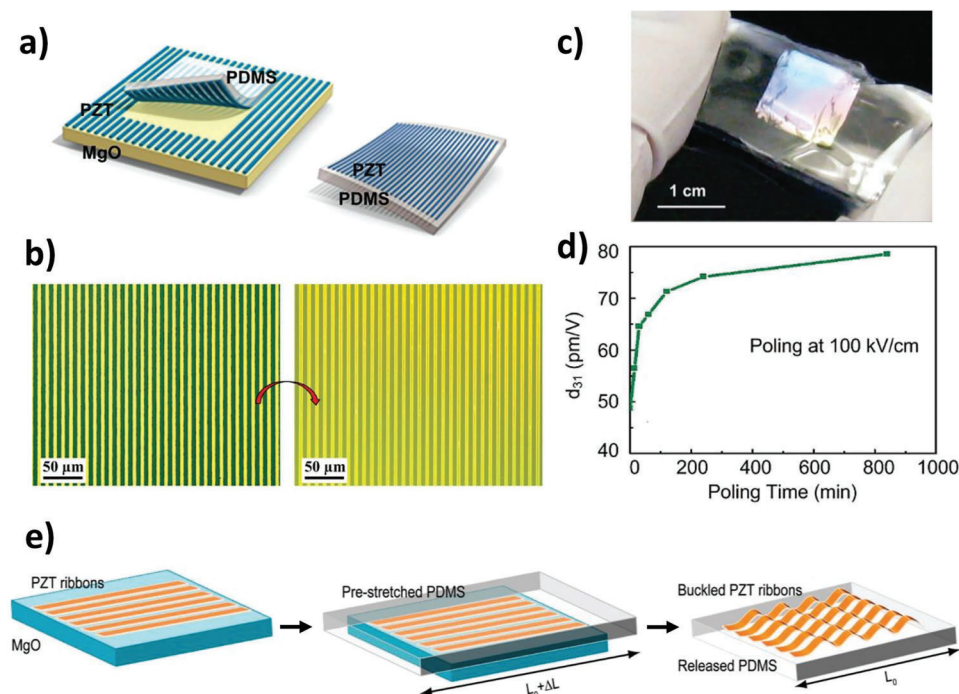


Figure 7. a) PZT ribbons synthesized on a MgO substrate, which is subsequently etched (left) and PZT ribbons are transferred onto a PDMS substrate (right). b) Optical image of PZT ribbons before and after transfer. c) Photograph of PZT ribbons on PDMS top surface. d) d_{31} at different poling times and a poling field of $\approx 100 \text{ kV cm}^{-1}$. Reproduced with permission.^[127] Copyright 2010, American Chemical Society. e) Formation of wavy/buckled piezoelectric PZT ribbons on a stretchable PDMS film in three steps from left to right: PZT ribbons on a sacrificial MgO substrate which is subsequently etched and transferred to a prestrained PDMS film. Reproduced with permission.^[128] Copyright 2011, American Chemical Society.

perturbation method was employed to rationalize mechanical stress transfer and corresponding induced polarization distribution within composites.^[137] The numerical data generated were in good agreement with reported experimental data revealing that the piezoelectric performance of 3D interconnected structures is an order of magnitude higher than randomly dispersed composite materials. The reason is that the interconnected structures create a continuous pathway for stress transfer within the 3D architecture. By contrast, the randomly dispersed composite relaxes and dissipates most of the stress within the soft matrix rather than transferring to the active ceramic phase.

3.2. All-Organic Elastomeric Compositing

This processing method technically considers only organic-based components in preparing composite materials. The strategy is based on incorporating polar organic or polymeric molecules with the tendency to retain a net macroscopic polarization into the elastic network of a nonpolar polymer matrix after poling. Usually, polymers with inherent polar crystalline domains, such as PVDF and its copolymers, odd-numbered nylons (nylon 7 and 11), etc., and polar amorphous polymers with glass-transitions (T_g) high above room temperature are used as active phase components.^[48] The dipolar segments in such active components, upon structuring, either by electrical poling or mechanical stretching, give rise to thermodynamically stable or quasi-stable oriented phases responsible for piezoelectricity. On the other hand, polymers that can maintain mechanical in-

tegrity by exhibiting recoverable strain deformations at different temperatures and frequencies, such as PDMS, etc., are used as matrices.^[138] Figure 9b gives a typical schematic representation of such composite material systems and the mechanism of generating polarization and piezoelectricity. When such a composite system is mechanically stretched or compressed, the dipole density changes due to fixed guest dipoles, leading to current flow.

Zhang et al. employed this processing technique in designing a flexible piezoelectric nanogenerator with a PVDF–PDMS composite material as the energy harvesting element.^[139] The process starts with manufacturing a mesoporous β -phase PVDF film by freeze-casting a solution of PVDF in dimethyl sulfoxide (DMSO) solvent. The DMSO is then sublimed at low pressure (0.8 Pa) at ambient temperature (18–25 °C). The resulting interconnected network with controlled porosity was infiltrated with PMDS solution and cured at an elevated temperature (70 °C). Following this simple but effective processing technique, the researchers demonstrated by basic electromechanical evaluations that the mechanical properties of the piezoelectric nanogenerator can be tailored to conform to biological tissues while maintaining an appreciable piezoelectric output. The tensile and compressive test revealed that the piezoelectric nanogenerator exhibits elastomeric behavior with Young's modulus as low as 0.8 MPa. The recorded modulus falls within the specified range for certain human organs, such as blood vessels, known to range from 0.1 to 1 MPa. Subjecting this device to 0.3 MPa compressive stresses at a frequency of 20 Hz gave an average open-circuit voltage of 2.87 V and a short-circuit current of 3.42 μA . An artificial artery system with this nanogenerator integrated into its

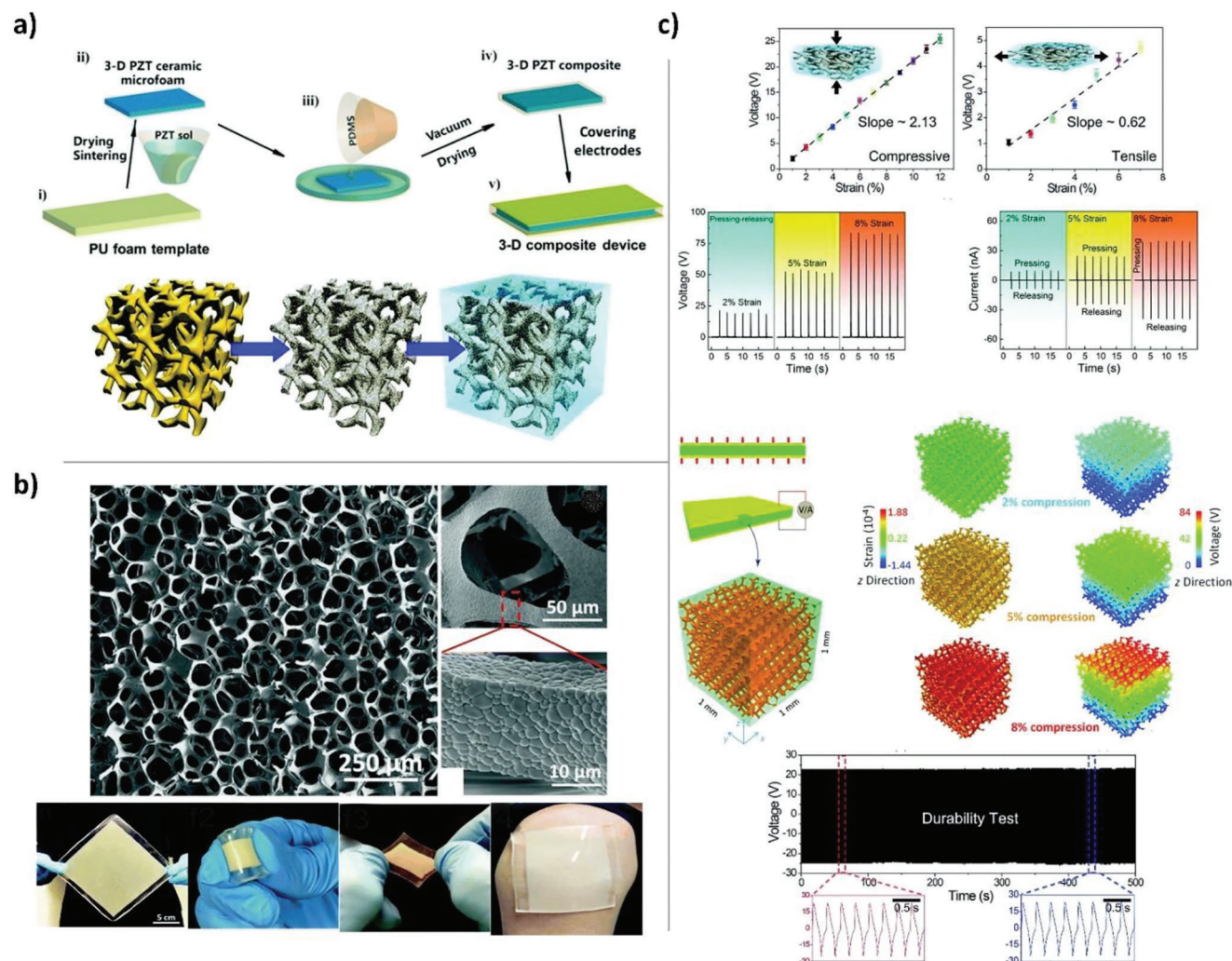


Figure 8. Fabrication and structures of the 3D ceramic–polymer composites. a) Representation of the composite preparation procedure. b) The SEM images of the macroporous ceramic skeleton and representative pictures of the composite demonstrate the possibility to bend and stretch by fingers and good conformation with the human body.^[106] c) Piezoelectric responses show output electrical signals under different compressive and tensile strains.^[106,137] Adapted with permission.^[106] Copyright 2018, Royal Society of Chemistry. Reproduced with permission.^[137] Copyright 2018, Royal Society of Chemistry.

fabrication further demonstrated the capabilities of harvesting mechanical energy from blood pressure fluctuations. By mimicking regular heartbeat activity, an average output voltage of 0.35 V could be achieved, proving potential application as a self-sufficient power supply for implantable devices. Mechanical mixing of PDMS with PVDF and CNT fillers allowed Hu et al. to achieve materials that gave a voltage of 2 V for PDMS/PVDF and 2.75 V for PDMS/PVDF/CNT, respectively. The functionality of the device was demonstrated by using the energy harvested to operate an LED.^[76] Park et al. reported a flexible and stretchable piezoelectric sensor consisting of poly(vinylidene fluoride-co-trifluoroethylene) electrospun nanofiber sandwiched between two elastomer films on which surface electrodes were sputtered. The developed sensors could be stretched and folded multiple times. Their functionality was demonstrated in a high-precision sensor and a skin-attachable pulse monitoring device.^[140] Duan et al. first made PVDF micro/nanofibers by combining helix

electrohydrodynamic printing and buckling-driven self-assembly and embedded them in PDMS to give highly stretchable generators. A peak current of 200 nA at 200% strain was measured when liquid-metal in PDMS served as electrodes.^[141]

In another communication by Moody et al., a design concept of doping nonpolar polymers with polar organic moieties proved a promising approach to fabricating flexible piezoelectric composite materials.^[142] The independent selection of matrix and dopant permits easy processing and tailorable properties. Thus, mechanical properties significantly depend on the choice of host matrix, while electric polarization relies on the selected dopant molecule. The dopant may not necessarily be inherently piezoelectric, but the possibility of creating long-range molecular ordering when incorporated into a polymer matrix unveils this synergistic piezoelectric behavior. Here, a highly polar 2-chloro-4-nitroaniline (CNA) molecule as a dopant was mixed with a polyurethane host matrix and, before cross-linking,

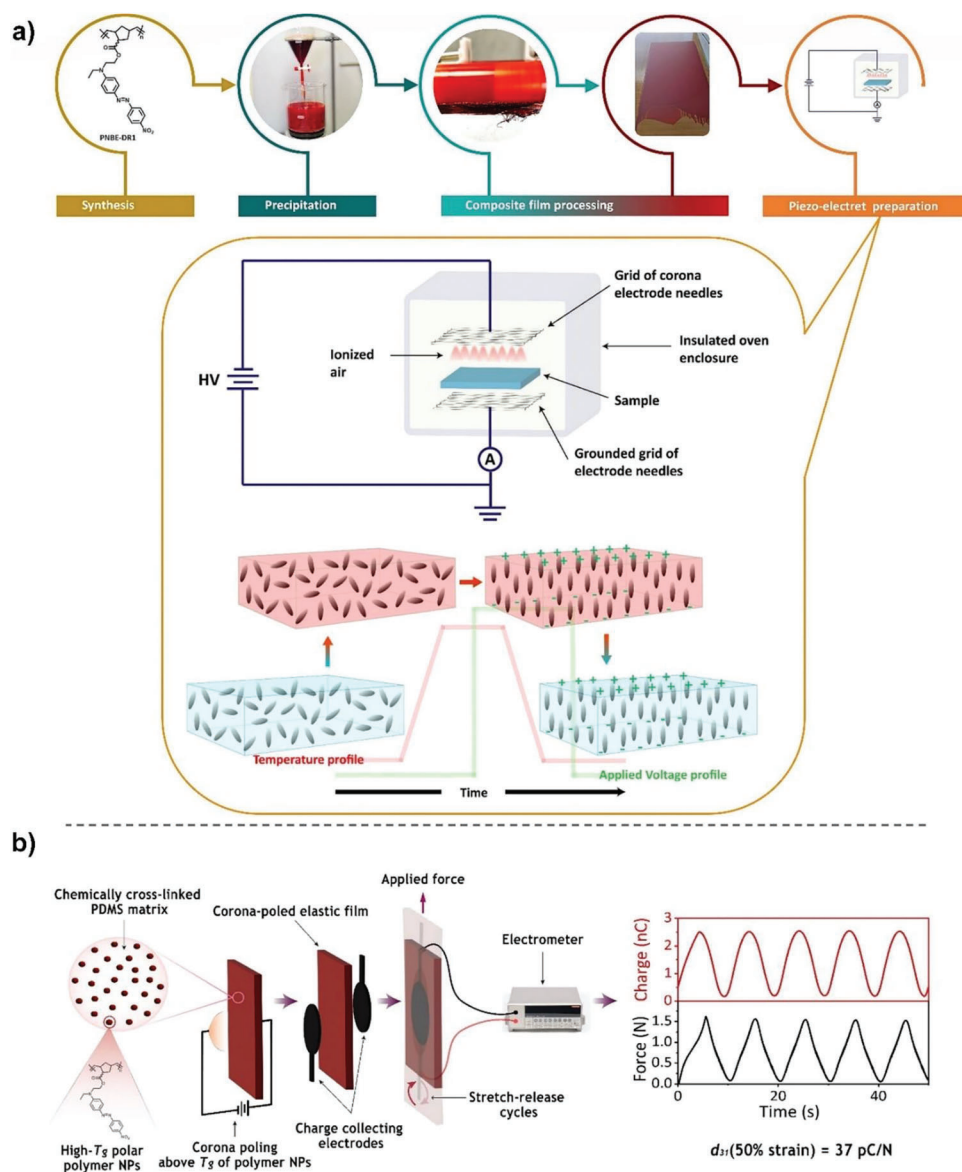


Figure 9. A typical approach for preparing all polymer-based piezoelectric elastomer. a) Flow diagram showing steps through synthesis and precipitation of polar polymer particles, processing into composites film with PDMS (using a three-roll-mill and blade casting), and corona poling in a strong electric field at elevated temperatures. b) Piezoelectric charge generation after poling. Adapted with permission.^[65] Copyright 2022, Wiley-VCH GmbH.

portioned into a poling fixture consisting of two electrodes. The sample mold was then cured at room temperature under an applied voltage bias. A quasi-static d_{33} piezocoefficient up to $244 \pm 30 \text{ pC N}^{-1}$ could be measured. Additionally, typical finger taps gave a peak current and power output of 5 nA and 5 nW, respectively. Nonetheless, the reported piezoelectric response showed strong dependence on the electric field applied during poling treatments, which also has an eventual effect on the stability of retained polarization. Thus, samples poled at low electric fields record piezoelectric coefficients decaying over orders of tens of minutes. Poling at a significantly higher electric field causes additional polarization stability, possibly conferred by the long-range cooperative effect, which delays the depolarization profile and the decay in piezoelectric response for days. The mechanism for a de-

crease in piezoelectric response over time is hypothesized to be caused by rotational diffusion of the dopants due to weak interfacial interactions between the dopant and host matrix, which then leads to depolarization. Larger dopants would likely improve stability by decreasing the rotational diffusion and increasing interaction with the matrix by cross-linking dopants into the polymer.

Underlying concepts of this processing technique have been further substantiated by the investigation works of Opris and co-workers. As illustrated in Figure 9a, a general workflow was followed as the design strategy for preparing piezoelectric elastomers. The first step involves the synthesis of polar amorphous polymers with T_g s considerably high above room temperature. Unlike inorganic ceramics, these amorphous polymers rely on the presence of molecular dipole units to exhibit piezoelectricity.

Besides, the dipoles should be oriented, stabilized in their aligned state and responsive to strain when mechanically stressed.^[48] The next steps require transforming these polar polymers into particles by solvent displacement technique, reinforcing them in an elastic PDMS matrix and blade casting into thin films. Finally, quasi-permanent polarization, responsible for the piezoelectric effect, is achieved by poling the films in a strong electric field at temperatures above the T_g of the filler particles. Under such conditions, the dipolar moieties orient in the direction of the electric field, and the achieved orientation is frozen-in by cooling the material back to room temperature with the field on. To maximize piezoelectric efficiency, the proposed system should retain sufficient polarization in the polar filler particles while maintaining low elastic modulus by the intrinsic property shown in the PDMS matrix. Preliminary experiments were conducted to prove this design concept in a typical sample, which was prepared using particles of a polar amorphous polymer, poly[(methyl methacrylate)-co-(Disperse Red 1 Methacrylate)] (P[(MMA)-co-(DR1MA)]) reinforced in a PDMS matrix. Mechanical properties of the resulting composite could be tailored to obtain an elastic modulus of 10 MPa, which is two orders of magnitude lower than that of commercial PVDF, and a strain at break of 300%. After electrode contact poling the prepared sample, the longitudinal piezoelectric coefficient (d_{33}) as a function of polarization was studied. The reported d_{33} values showed a quadratic growth from an amplitude of 3 to 27 pC N⁻¹ with increasing polarization.^[63] The same research group conducted further investigations to ascertain the stability of piezoelectric response in this material when operated in transverse (d_{31}) mode.^[64] The observed piezoelectric properties generally experienced a nonexponential decay revealing a strong onset decrease and a pseudostable state over one month study period. A stable transverse piezoelectric coefficient (d_{31}) as high as 12 pC N⁻¹ was recorded, which also proved to be thermally stable up to 50 °C.

To thoroughly understand the mechanism behind the time-dependent decay in piezoelectric response, a different polar amorphous polymer containing double bonds in its main chains was synthesized and introduced as filler in another study.^[65] The hypothetical reason behind this was to introduce enough rigidity into the molecular structure of the polar polymer, which may help limit dipolar relaxations possibly caused by a high degree of intramolecular chain rotations. Additionally, the contributing effects of filler particle size and filler–matrix interface on the eventual decay in remnant polarization were evaluated. Finally, the influence of the type of poling treatment on polarization and the eventual piezoelectric performance was studied. The published findings revealed piezoelectric properties with a similar decay profile as previously reported. Hence, the reason for introducing double bonds in the polar polymer main chains to limit depolarization could not be substantiated. This confirms that thermodynamic instability in oriented structures of polar amorphous polymers is a general intrinsic behavior.^[48] Immense theoretical simulations will be required to better understand these molecular dynamics. Concerning particle size variation, the piezoelectric response was reported to increase with decreasing particle size of the polar filler polymer. The observed behavior is likely due to effective stress transfer in composite systems with smaller filler particles than larger ones.^[143] Additionally, large interfacial boundaries in composites with smaller filler particles may

serve as charge traps to retain polarization. Another investigation was carried out to deconvolute the possible effect of interfacial relaxation on charge decay, which periodic mechanical strains may cause during operation. This was achieved by performing piezoelectric measurements on two samples that were processed under the same conditions. One was periodically strained for three weeks and the other left stands after poling. The recorded piezoelectric responses were similar, suggesting that charge decay in the prepared piezoelectric elastomer composite is not significantly influenced by the mechanism of mechanical deformation. Final studies also confirmed that samples subjected to corona poling treatment showed a threefold higher piezoelectric response than those treated with contact poling. A transverse piezoelectric coefficient of up to 37 pC N⁻¹ could be recorded for the best-performing material poled by corona discharge.

3.3. Porous Piezoelectret Elastomer by Foaming Techniques

Porous piezoelectret elastomer can also be considered a composite consisting of a gas phase dispersed in a solid polymer matrix. Thermoplastic polymers such as polyolefins, cyclo-olefin polymers and their copolymers, PU, polyvinyl chloride, poly(ethylene terephthalate), poly(ethylene naphthalate), and fluoropolymers have commonly been used in the preparation of such cellular materials. The technique presents a simple and easy way of preparing flexible and stretchable materials with outstanding electromechanical behavior. Processing requires a combination of foaming and poling methods. Foaming is generally performed by mechanical, physical, and chemical means, which is sometimes coupled with extrusion and injection molding processing techniques.^[89,144,145] Alternatively, cellular materials can be achieved by sugar-templating strategies and stretching particulate-filled polymers to initiate voids at the filler–polymer interfaces through delamination.^[146,147] Piezoelectricity can be induced in such voided materials by ionizing the air pockets by applying a sufficiently high electric field. This can be achieved through direct electrode contact poling, corona discharge poling, or soft X-ray poling. A typical preparation procedure is schematically represented in **Figure 10**.

The inner Townsend breakdown triggers whenever the applied charging voltage exceeds a specific threshold value and is responsible for charge deposition in the voids, as shown in **Figure 10c**.^[89] Trapped charges with opposite polarities are then formed on the voids' interior upper and lower surfaces, creating a dipole-like macroscopic structure. Such compliant polymers, also termed piezoelectrets or ferroelectrets, containing polarized cavities can respond to electrical or mechanical stimuli similar to the piezoelectric material. Analogous to a displacement of ionic or molecular dipoles in a regular piezoelectric material, the deformation of the charged voids is the cause of the piezoelectric effect. Following a sequence of well-designed preparation steps, the thermal stability, annealing history, dimension, shape, and porosity of resulting foamed materials affect piezoelectric response.^[89,148] Since there is a need to maintain polarization in the charged pores, the polymer should ideally be a good dielectric, electrically insulating, and able to retain trapped charges.

Fang et al. reported a cellular PEN piezoelectret fabricated from a commercial PEN polymer film through physical foaming

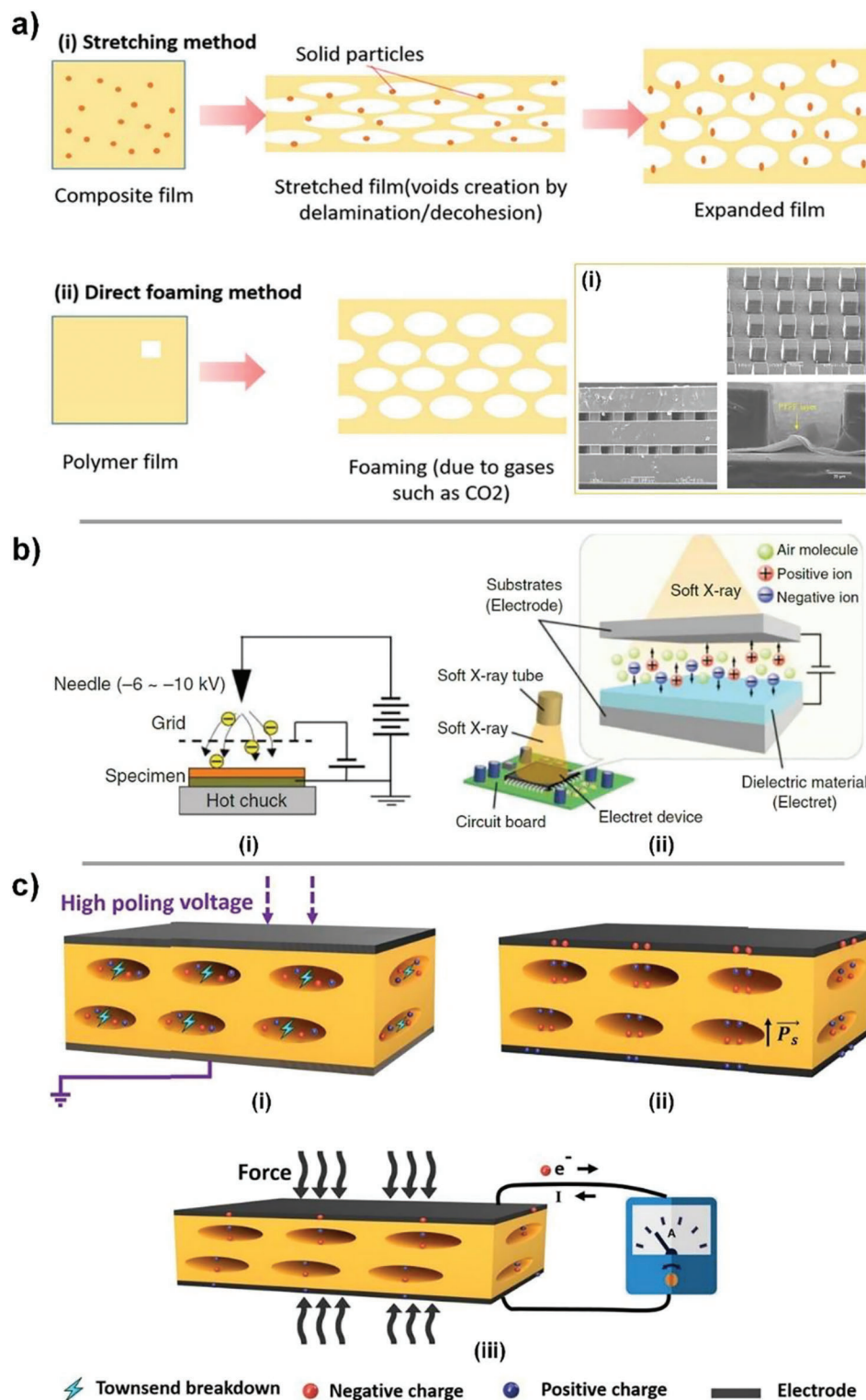


Figure 10. Schematic illustration of the preparation and working mechanism of cellular piezoelectrets. a) Route of foaming. Reproduced with permission.^[147] Copyright 2022, Wiley-VCH GmbH. (i) SEM images of the top view, cross-sectional view, and close view of cellular PDMS microstructures. Reproduced with permission.^[154] Copyright 2014, Elsevier. b) Electric poling methods (i) typical corona charging system and (ii) through-substrate soft-X-ray charging. Reproduced with permission.^[153] Copyright 2015, Wiley-VCH GmbH. c) Mechanism of piezoelectret operation (i) Townsend breakdown under a high poling voltage following Paschen's law for a breakdown in air, (ii) charged sample having positive/negative electrical charges on the opposite faces of the polymer surfaces with the polarization of P_s , and (iii) piezoelectrically induced charge flow when an external force applied along the polarization direction. Reproduced with permission.^[89] Copyright 2019, Elsevier.

in supercritical carbon dioxide (scCO₂), inflation, biaxial stretching, and electrical charging.^[148,149] The PEN film was initially soaked in scCO₂ at high pressure (150 bar) for a few hours. The scCO₂-saturated polymer was then subjected to heat treatment for a few seconds at a temperature above the T_g of PEN. The sudden increase in the volume of the scCO₂ fluid upon phase change led to the foaming of the film. Subsequently, the voided film was inflated by exposing it to high-pressure gas until the voids were sufficiently filled with pressurized gas and further heat treated to improve the cellular geometry. After inflation, the foamed PEN film was subjected to biaxial stretching to decrease void heights and change geometry to lens-shaped voids. Electrical charging of the voided film was achieved by either electrode contact poling or corona discharge poling under different poling conditions. Piezoelectricity arises from the combination of internally separated and trapped charges and anisotropy in the cellular polymer matrix with very low elastic stiffness. The densities of the prepared foamed PEN films and the poling conditions influenced the reported piezoelectric coefficients (d_{33}). Thus, relatively high d_{33} coefficients could only be achieved in samples with an optimal density $\approx 1.1 \text{ g cm}^{-3}$ and lower elastic stiffness. Generally, samples charged under higher voltages gave off a stronger piezoelectric response. The contact-poled samples exhibited low piezoelectric properties compared to the corona-poled counterparts. Piezoelectric d_{33} coefficients up to 140 pC N^{-1} , which proved thermally stable until 80°C could be achieved. Additionally, samples poled at elevated temperatures below T_g show improved thermal stability in terms of their piezoelectric response than those poled at room temperature.^[148]

In another preliminary communication, Galantini et al. presented a piezoelectric elastomer fabricated using cellular polyurethane films and charging by the corona process.^[150] The foamed films were prepared via mold casting of an emulsion containing liquid polyurethane precursors (diisocyanate and polyol) and a preoptimized ratio of distilled water (10 wt%) suitable for designing porous structures with excellent elasticity and dielectric properties. The molded films were sufficiently cured at ambient temperature for 2 days and subsequently at elevated temperature (60°C) under vacuum for 24 h. An adequate enough processing voltage (4.5 kV) was precautionarily applied to corona-charge the prepared cellular samples, and the induced electromechanical properties were evaluated. Wang et al. made a $300 \mu\text{m}$ thick cellular PDMS structure with micrometer-sized voids internally coated with a thin polytetrafluoroethylene (PTFE) sandwich between two stretchable gold electrodes. An electric field of up to 35 mV m^{-1} was applied to ionize the air in the voids and inject charges onto the inner voids surfaces. The resulting structure is stretchable, has an elastic modulus of $\approx 300 \text{ kPa}$, a stress sensitivity of $\approx 10 \text{ mV Pa}^{-1}$, and shows a piezoelectric coefficient d_{33} of $\approx 1000 \text{ pC N}^{-1}$.^[151] Lacour et al. made a stack of ten polypropylene films consisting of alternating positive/negative charged cellular polypropylene films with a $d_{33} = 200 \text{ pC N}^{-1}$ glued by thin PDMS layers sandwiched between two stretchable electrodes. This piezoelectric device was compliant with human skin and exhibited good pressure sensitivity.^[152]

Zhong et al. designed a sandwich-structure piezoelectret composed of two fluorinated ethylene propylene electret films, which sandwich an Ecoflex film with holes as a spacer. The electrical connections were made using a gold (Au) and an aluminum (Al)

electrode on the top and bottom of the piezoelectret, respectively. A piezoelectric coefficient as high as 4050 pC N^{-1} and a stable response was reported.^[155] Tsai et al. developed cellular PDMS films internally coated with a thin layer of PTFE. The charges generated in the voids during poling are deposited on the PTFE. The designed structure showed an elastic modulus of about 300 kPa and a piezoelectric coefficient d_{33} of $\approx 1500 \text{ pC N}^{-1}$.^[154] Similarly, Kachroudi et al. made microstructured cellular PDMS with an area of $2 \times 2 \text{ cm}^2$ and a total thickness of $150 \mu\text{m}$ consisting of two bulk layers separated by the microstructured one and coated with two gold electrodes and charged it at 1 and 4 kV and a frequency of 0.5 Hz . The device showed a piezoelectric coefficient d_{33} of 350 pC N^{-1} , which is ten times larger than polyvinylidene fluoride.^[155] Recently, Hu et al. used the sugar-templating method coupled with corona poling to design a soft and stretchable piezoelectret with outstanding electromechanical behavior.^[156] The porous material was first prepared by simply mixing a solution of silicone-based elastomeric kit (Sylgard 184 PDMS) in proportionate amounts with PTFE fillers and sugar particles. The resulting viscous mixture was mold-cast and sufficiently cured at elevated temperatures. The cured mold was repeatedly soaked in warm water to dissolve the sacrificial sugar template and oven-dried thereafter. Uniformly distributed porous structures, composed of PTFE particles immobilized in the PDMS matrix, were obtained and the extent of porosity could be tuned by the amount of sugar particles added. Following electrical treatment, the pores are internally charged, generating “pseudo” macroscopic dipoles. The direct piezoelectric coefficient was evaluated by a quasi-static and dynamic method. A quasi-static piezoelectric coefficient (d_{33}^{eff}) up to 477 pC N^{-1} could be attained when the polarized porous piezoelectret was subjected to 5 N external load. The piezoelectric performance was proven to strongly depend on the PTFE filler content, the extent of polarization, which directly informs the number of macroscopic dipoles generated, porosity and the charge retention capabilities of the piezoelectret, and the measuring frequency. As reported, the d_{33} coefficient was almost stable after a week of periodic measurements. Ma et al. made a porous structure by mixing a PDMS matrix with PZT particles and NaCl powder, whereby the NaCl powder served as a sacrificial filler. The formed composite was polarized at an electric field of 1.6 kV mm^{-1} . A generator with dimensions of $2 \times 2 \times 0.3 \text{ cm}^3$ gave an open-circuit voltage of 29 V and a short-circuit current of 116 nA under 30 N .^[157] For a more detailed review of the potential of porous materials for energy harvesting and processing routes to porous electrets, the reader is referred to a recent review on this topic.^[93]

3.4. Intrinsic Piezoelectric Elastomer Synthesis

Organic synthetic methods have also been employed in the de novo design and processing of elastomers with piezoelectric properties. The strategy used here is to carefully select reaction pathways from the organic toolbox that can eventually affect structural modifications and long-range intermolecular assembly of dipolar moieties when an electrical or mechanical stimulus is applied. Molecular structure illustrations of elastomers with intrinsic piezoelectric behavior can be found in **Figure 11**.

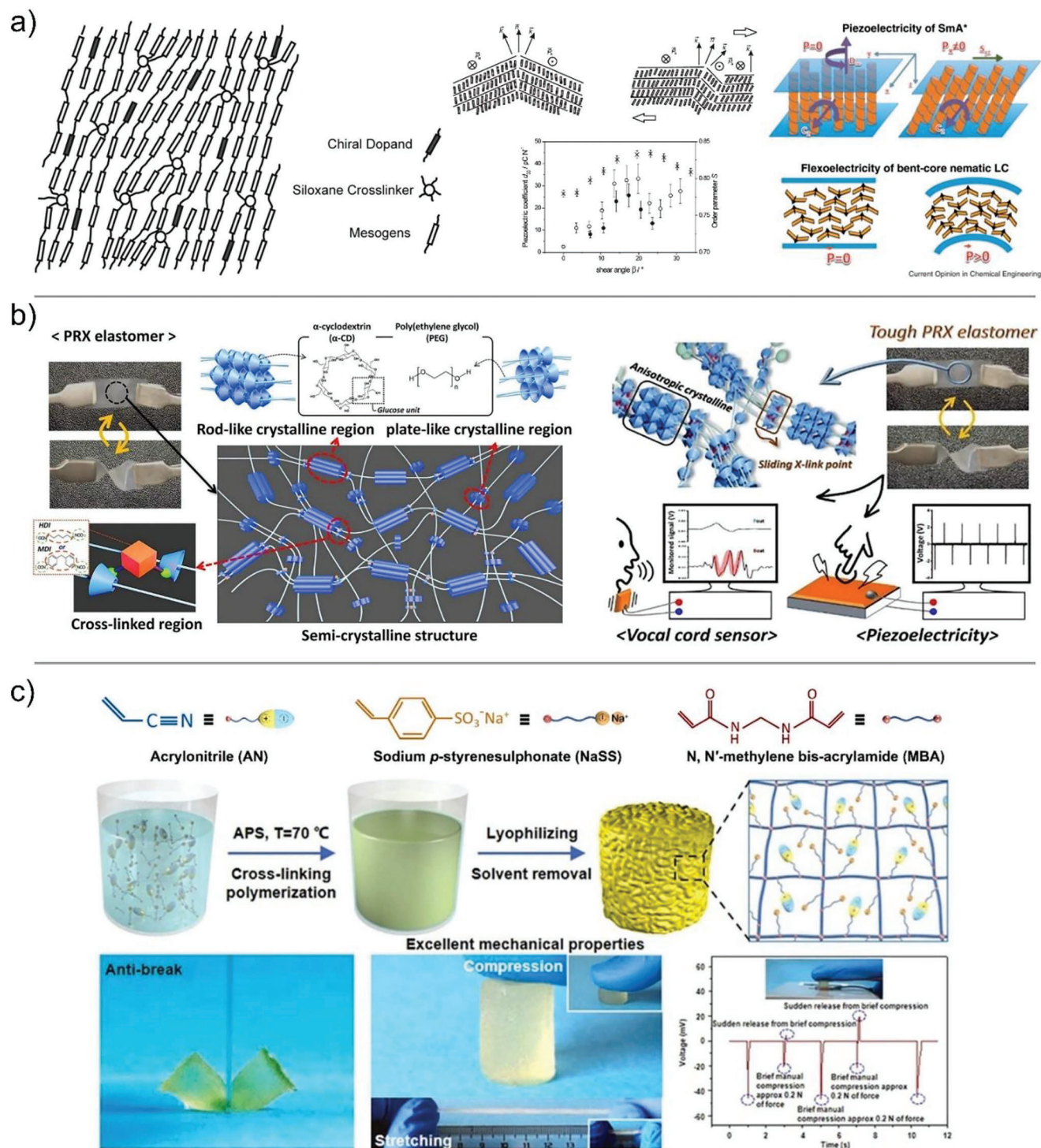


Figure 11. Schematic illustration of the molecular structures of elastomers with intrinsic piezoelectric behavior and the physical mechanism for generating piezoelectricity. a) Structural representation of main-chain smectic C* LCs. Achiral dopant is added to induce the formation of domains with a permanent electric dipole moment. Effects of shear on making the elastomer piezoelectric by phase conversion reflect in the increase of the piezoelectric coefficient. Reproduced with permission.^[173] Copyright 2010, American Chemical Society. Reproduced with permission.^[174] Copyright 2013, Elsevier. b) Internal structure of PRX elastomers composed of ring-shaped α -CD host molecules threaded on linear PEG guest polymer chains and representation of electrical signal generated by voice pitch and finger touch. Reproduced with permission.^[175] Copyright 2021, Elsevier. c) Fabrication procedure for poly(sodium *p*-styrenesulphonate-co-acrylonitrile) copolymer cross-linked network with representative photographs and electric signal generation. Reproduced with permission.^[176] Copyright 2022, Elsevier.

One of the earliest preliminary studies on the synthesis of elastic materials which exhibit intrinsic piezoelectricity was conducted by Zentel in the late 1980s.^[158–161] A consideration based on incorporating mesogenic molecular moieties in polymer main chains and/or as side groups and cross-linking into liquid crystalline elastomers (LCEs). Synthetic techniques used, thus far, in fabricating LCEs include free radical copolymerization of acrylates or methacrylates,^[162,163] hydrosilylation of silicon hydride and alkene,^[164–166] azeotropic or melt polycondensation of diols with allylmalonic acid or diethyl allylmalonate, polyaddition of epoxy and carboxylic acid,^[158,167,168] and other reactions involving click chemistry. Li et al. recently published a comprehensive review of emerging synthetic approaches to LCEs.^[169] LCEs combine the orientability of mesogenic groups into ordered liquid crystalline (LC) phases with elasticity and flexibility inherent to rubbers. Piezoelectric properties can be achieved depending on the chirality of the mesogens and the retained LC phases in the LCEs. Thus, applying sufficient mechanical stress to these cross-linked elastomers causes conformational changes in the polymer main chains and effects reorientation in the LC phase. This eventually can transform the chiral phase with zero net polarization into structures with macroscopic polarization making them promising materials in electro-optics, energy harvesting, flexible electronics, and actuator technologies.^[160,170–172]

In 2010, Heinze et al. investigated a homologous series of chiral LCEs to understand further how varying amounts of chiral dopant influenced the crystal phase ordering and the electromechanical properties. Hydrosilylation step-growth reaction was employed to synthesize chiral smectic C* main chain LCEs, with chirality achieved by doping a smectic C host system. The effect of shear stress in reorienting the LC phase was studied by measuring spontaneous polarization and X-ray diffraction. Generally, exposure to shear deformation caused a macroscopic realignment of the chiral Smectic C* phase leading to electric polarization. The formation of charges on the elastomer surface due to polarization was linearly dependent on smaller shear angles with an onset of a distant nonlinearity above 25° angle. Additionally, the measured spontaneous polarization showed a linear dependence on the amount of chiral dopant with a value up to 370 $\mu\text{C m}^{-2}$ attainable. That is to say, doping LCEs with chiral mesogens induce the formation of domains with permanent electric dipole moments, which cause them to exhibit piezoelectric properties.

Following this publication, Papadopoulos et al., in the same year, studied further the piezoelectric behavior on one of the doped smectic C* liquid crystal elastomers as a function of shear, static mechanical stress, frequency, and temperature.^[173] The investigation confirmed that processing by shear effectively produces electromechanically active LCEs and the exact set shear parameters are crucial in realizing optimal performance. The optimum direct piezoelectric coefficient ($d_{33} = 35 \text{ pC N}^{-1}$) was measured for samples processed at a shear angle of 22°, which is in agreement with the report by Heinze et al. Although the reported elastic modulus was almost independent of frequency over three decades (1–1000 Hz), the d_{33} value shows a clear decrease with increasing frequency. This is attributed to large mechanical losses at frequencies above 10 Hz. The elastomer exhibited a constant d_{33} value with increasing static mechanical stress up to $\approx 0.3 \text{ MPa}$ (corresponding to a static strain deformation of $\approx 3\%$) but decreased drastically thereafter. The plummeting electromechani-

cal response at larger static deformations is ascribed to distortion in the morphology of the LC phase monodomain. Furthermore, the elastomer showed an increasing d_{33} response as a function of temperature until the smectic C*-to-isotropic phase transition is reached, after which a sharp irreversible drop is observed. In summary, the d_{33} value does not change by more than a factor of 2 within a broad frequency, temperature, and static deformation range.

A recent study by Zhou and co-workers unveiled another technique to fabricate elastomers with inherent piezoelectric properties.^[176] This facile process involves a one-pot free radical cross-linking copolymerization of acrylonitrile, sodium p-styrene sulphonate, and N-ethylene bisacrylamide in DMSO, which yielded a poly(sodium p-styrenesulphonate-co-acrylonitrile)organogel. The organogel was then freeze-dried to remove DMSO and form an elastic copolymer network with highly polar groups. The structural morphology could be retained due to the electrostatic repulsion and spatial resistance caused by the sodium p-styrene sulphonate ionic monomer coupled with the loosely cross-linked network induced by freeze-drying. This eventually limits the possibility of intermolecular dipolar interactions of the acrylonitrile units and enhances the internal mobility of the highly polar nitrile side groups. Subjecting this elastomer to mechanical deformation facilitates change in polarization due to dipole movement and rotation from the randomized zero net polarization equilibrium position to a nonzero net polarization state. Thus, the bulk elastomer can be easily polarized by mechanical stress courtesy of its low Young's modulus and the abundant interspaced nitrile side groups with high polarity. The fabricated soft tissue-like elastomer could therefore display excellent electromechanical behavior with an appreciably high piezoelectric charge coefficient of 40 pC N^{-1} and a recoverable elasticity under 100% strain. Additionally, this elastomer exhibited a fast and stable electrical response, good mechanical damping qualities, and excellent sensitivity attributed to the stress-induced polarization behavior inherent to the material. Due to this material's elastic and piezoelectric responsiveness, it has been demonstrated and proposed for application as a potential artificial skin for simultaneous impact protection and self-sensing, as well as continuous human pulse monitoring.

Functionally graded polyrotaxane (PRX) elastomers composed of ring-shaped α -cyclodextrin (α -CD) host molecules threaded on linear poly(ethylene glycol) (PEG) guest polymer chains have also been demonstrated to exhibit piezoelectric effect by Seo and co-workers.^[175] This polymer was cross-linked with diisocyanates via urethane bond formation by taking advantage of the hydroxyl groups on α -CDs. The elastic properties could be tuned by the type and amount of cross-linker used. Among the non-crosslinked adjacent α -CD bundles, the PRX polymer chains could associate through hydrogen bonding to form hexagonally packed anisotropic crystalline domains. The level of anisotropy and crystallinity, which is informed by the blend ratio of PRX polymers with different chain lengths, determines the piezoelectric activity. Meanwhile, the partially cross-linked α -CD molecules maintain a "slide-ring" pulley effect responsible for the mechanical integrity of the elastomer. The PRX elastomer was therefore reported to show superior mechanical properties comparable to commercially available PDMS and piezoelectric charge coefficient (d_{33}) of 7 pC N^{-1} . A piezoelectric device fabricated from the

Table 1. Overview of different piezoelectric elastomers from literature, including the elastic matrix and filler used, filler's connectivity, dielectric permittivity, and piezoelectric constants.

Matrix	Filler	Connectivity	ϵ_r	Y [MPa]	Piezoelectric constants	Refs.
Chloroprene rubber	60 vol% PZT	0–3	100	–	$d_{33} = 46 \text{ pC N}^{-1}$ $d_{31} = -14 \text{ pC N}^{-1}$ $g_{33} = 35 \text{ mV m N}^{-1}$ $g_{31} = -11 \text{ mV m N}^{-1}$	[103]
Poly(acrylonitrile butadiene) rubber	80 vol% PMN	0–3	110	–	$d_{33} = 33 \text{ pC N}^{-1}$	[107]
PDMS	43 vol% PZT	0–3	21	4	$d_{33} = 6.8 \text{ pC N}^{-1}$ $d_{31} = 48 \text{ pC N}^{-1}$	[112]
Rubber	92 wt% PZT	0–3	–	5	–	[113]
PDMS	6 vol% structured KNLN	1–3	7	–	$d_{31} = 35 \text{ pC N}^{-1}$ $g_{33} = 510 \text{ mV m N}^{-1}$	[94]
PDMS	8 vol% structured BCZT	1–3	6	–	$d_{33} = 31 \text{ pC N}^{-1}$ $g_{33} = 600 \text{ mV m N}^{-1}$	[97]
PDMS	50 vol% PZT	1–3	–	–	$d_{33} = 101 \text{ pm V}^{-1}$ $d_{31} = 79 \text{ pm V}^{-1}$	[119]
PDMS	20–60 vol% PZT	3–3	40–200	22–27	$d_{33} = 80\text{--}240 \text{ pC N}^{-1}$	[124–127]
CNA-doped polyurethane foams	–	–	–	–	$d_{33} = 244 \text{ pC N}^{-1}$	[134]
PDMS	33–40 wt% poly [(MMA)- <i>co</i> -(DR1-MA)]	–	3	4.7	$d_{33} = 27 \text{ pC N}^{-1}$ $d_{31} = 12 \text{ pC N}^{-1}$	[63,64]
PDMS	30 wt% polar polynorbornene	–	5	4.6	$d_{31} = 37 \text{ pC N}^{-1}$	[65]
Cellular PEN	Air	–	–	1.4	$d_{33} = 140 \text{ pC N}^{-1}$	[140, 141]
Porous PDMS	Air	–	–	0.3	$d_{33} = 1000\text{--}1500 \text{ pC N}^{-1}$	[143, 146]
PDMS sponge	Air	–	–	0.2	$d_{33} = 477 \text{ pC N}^{-1}$	[148]
Microstructured cellular PDMS	Air	–	–	0.3	$d_{33} = 350 \text{ pC N}^{-1}$	[55]
Smectic C* liquid crystal elastomers	–	–	–	12	$d_{33} = 20 \text{ pC N}^{-1}$	[165]
P(NaSS- <i>co</i> -AN) elastomer	–	–	–	0.2	$d_{33} = 40 \text{ pC N}^{-1}$	[168]

elastomer with optimal characteristics gave a stable open-circuit voltage of 3.7 V, a current density of 360 nA cm^{-2} , and a power density of $1.34 \text{ } \mu\text{W cm}^{-2}$ upon repeated cyclic test. The scientists then attached this device to a nose mask and reported an enhanced piezosensitivity against the mechanical vibrations generated by respiratory signals proving the novelty of employing this smart elastomer as an energy harvester.^[175,177] da Cruz et al. made a collagen blend in 10% natural rubber. While the d_{14} of the blend decreased from 0.057 pC N^{-1} for neat collagen to 0.042 pC N^{-1} , the addition of NR increased the thermal stability.^[178] Also, a polyurethane elastomer poled at 25 mV m^{-1} was reported to show a d_{31} of 184 pC N^{-1} .^[179] Unfortunately, polyurethanes are a broad class of polymers; thus, it is difficult to determine the exact molecular composition exhibiting outstanding properties.

Chitosan has a noncentrosymmetric crystal structure; therefore, solution-casted chitosan films have a piezoelectric response of 6 pC N^{-1} .^[180] Its piezoelectric response could be enhanced by neutralization to reach a value as high as 16 pC N^{-1} .^[181] However, chitosan is flexible, but not stretchable. Appropriate manufacturing and device engineering may allow stretchability.^[182]

Different elastic matrices and active fillers have been used to synthesize piezoelectric elastomers. Table 1 gives an overview of some piezoelectric elastomers reported in the literature and their

piezoelectric response. The most explored elastic matrix is based on PDMS, likely due to easy processability and cross-linking. While some materials show promising responses, more research has to be conducted to find their long time stability under different humidity and temperature conditions.

By far, the highest piezoelectric response was found in charged porous elastic insulators, with values as high as 1500 pC N^{-1} . Such materials also have a rather low elastic modulus. However, humidity and temperature may affect their long time performance. Additionally, efficient and scalable processes for such porous structures need to be found. Composites with a 3–3 connectivity and high piezoactive filler content also show a strong piezoelectric response with values reaching 240 pC N^{-1} . However, the elastic moduli of such composites increase with filler content, which may be problematic for implants. Additionally, most ceramic fillers are lead based and thus, toxic. All organic piezoelectric elastomers have a relatively low elastic modulus, but their piezoelectric response is lower than that of ceramic composites and porous elastomers. Recent work showed that carefully selecting filler material and poling could increase the piezoelectric response. Corona poling allows for higher electric fields in the poled material, as it tolerates more defects. While significant research was invested in developing improved piezoelectric

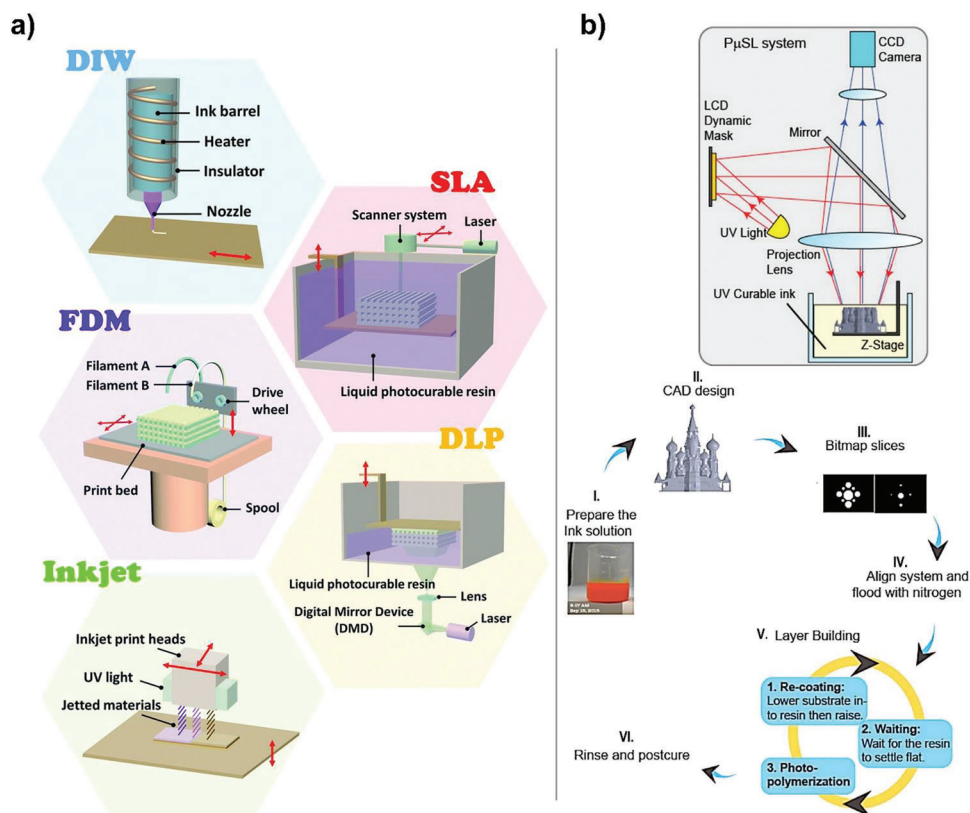


Figure 12. Schematic illustration of additive manufacturing techniques. a) Extrusion-based direct ink writing (DIW) and fused deposition modeling (FDM) form 3D projects in a line-by-line and then layer-by-layer manner. Photopolymerization-based stereolithography (SLA) and digital light processing (DLP) can print in sub-micrometer resolution with high fidelity. SLA employs a laser beam and scanner system, while DLP relies on a digital mirror device (DMD) to achieve dynamic pattern generation. Inkjet printing uses a thermal or piezoelectric actuator to jet materials. Reproduced with permission.^[186] Copyright 2022, Royal Society of Chemistry. b) A typical projection micro-stereolithography (PμSL) system and the 3D printing process flow. Reproduced with permission.^[191] Copyright 2017, Elsevier.

elastomers, little is known about how the electrode material used influences the amount of charge collected. Future work should address this issue.

3.5. Additive Manufacturing

The underlying concept of this processing technique can be dated back to the invention work of Charles Hull in 1986, which paved the way for designing complex architectures from printable functional materials. Generally, additive manufacturing refers to fabricating 3D complex structures via controlled deposition of materials in printable ink forms. The inks employed include metals, ceramics, polymers, and their hybrid blends. The operation begins with designing 3D virtual models segmented into numerous 2D horizontal cross-sections based on computer-aided design (CAD) software. Successive printing of a new 2D layer on top of previous layers leads to the fabrication of a coherent 3D object.^[14,183] Further extensions known as 4D printing, which considers time-dependent variables to trigger printing through external stimuli such as electromagnetism, temperature, pH, and light, have also been reported.^[184–186] The technique serves as a big umbrella that describes several processes of constructing designed parts in a layer-by-layer fashion. These include stere-

olithography, selective layer sintering, direct ink writing, solvent evaporation-assisted 3D printing, fused deposition modeling, digital light processing, electric poling-assisted additive manufacturing, two-photon polymerization, and many more. Two-photon lithography allows the manufacturing of complex 3D structures with a resolution of 100 nm or better.^[187] The abundant photore-sists with different properties and the possibility of combining them with piezoelectric fillers may open the doors to intriguing applications.^[188]

Figure 12a shows graphical representations of some additive manufacturing techniques. A detailed description of these processes can be found in other reviews.^[14,189,190] The technology has gained widespread application due to its advantages, such as low manufacturing cost, high material utilization, production precision, and the absence of structural restrictions during printing.

Additively assembled piezoelectric elastomers are gradually gaining popularity for their optimized application in sensors, actuators, energy harvesters, and tissue engineering.^[192–194] Sun and co-workers recently developed a piezoelectric polymer photocurable ink suitable for 3D printing by projection micro-stereolithography (PμSL) processing technique.^[191] The formulated ink contained PDVF particles as the piezoactive phase, 1,6-hexanediol diacrylate monomer as a matrix, Irgacure 819 as a photoinitiator, Sudan I as a UV absorber, and diethyl fumarate as

a solvent to adjust the viscosity. Considering a trade-off between manufacturability and piezoelectric characteristics, the ink could be optimized to contain 35 wt% PVDF, 40 wt% 1,6-hexanediol diacrylate, 2.2 wt% photoinitiator, 0.12 wt% UV absorber, and 22.68 wt% solvent. A schematic illustration of the PuSL system and the 3D printing process flow is shown in Figure 12b. Following a 3D CAD model, the substrate on which the printing is to be made is vertically mounted and aligned with a movement precision of 0.5 μm . The printing process is then initiated and after depositing each layer, the resin is exposed to UV light via a dynamic mask to cure in a controlled photopolymerization fashion. By repeating these steps for each layer, complex 3D structures with customized geometries could be rapidly designed. On completion, the fabricated device was rinsed in diethyl fumarate to remove the uncured residues and further exposed to UV irradiation to cure the structures completely. A piezoelectric voltage coefficient (g_{33}) of 105 mV m N⁻¹ following a poling treatment was reported, comparable to that of pure PVDF film.

4. Summary and Future Perspective

The rapid technological advancement toward a more humane future increasingly demands energy harvesters, sensors, and actuators that can be easily integrated into devices. In respect to this, piezoelectric materials with improved elastic integrity, excellent electromechanical transduction effect, ease of processing, and pliability at complex interfaces, among other advantages, become relevant aspects. Approaching such materials from the design perspective will concurrently require looking into the fabrication methods. We have therefore presented a concise overview of processing techniques adopted for the development of piezoelectric elastomers. The history and fundamental mechanisms of piezoelectricity from the materials' viewpoint have been briefly discussed. The article shows that the performance of piezoelectric elastomers can be enhanced through effective processing strategies. Compositing techniques have been employed in fabricating stretchable hybrid materials, which take advantage of the elastic properties of elastomer matrices and the piezoelectric behavior of the filler. However, designing such materials to give properties beyond the sum of the individual components' properties requires significant effort in creating materials, optimizing fabrication conditions, and understanding the structure–property relations. For instance, ceramic–polymer-based composite materials prepared by random dispersion of ceramic fillers in the elastic matrices often result in limited connectivity. Hence, issues pertaining to permittivity mismatch between the two phases arise, which result in nonuniform electric field distribution when poling. This causes weak levels of polarization and piezoelectric activity. Higher connectivity of the ceramic phase can be achieved with dielectrophoresis and 3D interconnected structures designed from sacrificial templates. Although higher dimensional connectivity of the ceramic component results in impressive piezoelectric performance, they are restricted when subjected to high mechanical strains. Therefore, the trade-off between elasticity and piezoelectricity will demand more structural insight into the composites to understand further the interfacial effect to gain. Such interfacial layers can impact the piezoelectric response through friction and contact electrification at polymer interfaces giving rise to a triboelectric–piezoelectric response. Ex-

tracting the piezoelectric charge from a hybrid signal is challenging, especially in composites, but may allow a better understanding of the structure–property relationship and a more fair and correct analysis of different piezoelectric materials. Sutka et al. have described in detail how to distinguish these effects and have reviewed the literature on deconvoluting the piezo- and triboelectric outputs.^[96]

Therefore, careful domain and interfacial engineering may assist in designing composites with intriguing performance. Other processing strategies discussed have likewise achieved a certain level of development, but intrinsic material characteristics and availability are bottlenecks for implementation. For example, the emergence of additive manufacturing provides new advantages for integrating piezoelectric elements into devices by eliminating tedious assembly and packaging steps during fabrication to improve manufacturing efficiency and performance of the device. However, the technology is not very matured for piezoelectric elastomer materials and still limited to experimentation and prototyping. It is, therefore, necessary to discover materials that can withstand processing conditions and, at the same time, present high performance. The authors are convinced that problems faced in developing piezoelectric elastomer materials can be solved by careful materials design and processing, bringing these materials closer to application.

Acknowledgements

This work received funding from the Swiss National Science Foundation (I.Z.S.A.Z.2_173358/1 and 206021_150638/1), the Swiss Federal Laboratories for Materials Science and Technology (Empa, Dübendorf, Switzerland), and the European Research Council (ERC) under the European Union's Horizon 2020 research and innovation programme (Grant Agreement No. 101001182).

Open access funding provided by ETH-Bereich Forschungsanstalten.

Conflict of Interest

The authors declare no conflict of interest.

Keywords

electret elastomers, electrical poling, foams, piezoelectric elastomers, pressure sensors

Received: January 24, 2023

Revised: April 22, 2023

Published online: June 17, 2023

- [1] W. Heywang, K. Lubitz, W. Wersing, in *Piezoelectricity: Evolution and Future of a Technology*, Springer Series in Materials Science 114, Springer, Berlin **2008**.
- [2] H. S. Nalwa, *Ferroelectric Polymers: Chemistry, Physics, and Applications*, CRC Press, xx **1995**.
- [3] S. Bauer, F. Bauer, in *Piezoelectricity: Evolution and Future of a Technology*, Springer, Berlin **2008**, p. 157.
- [4] F. Carpi, D. De Rossi, R. Kornbluh, R. Pelrine, P. Sommer-Larsen, *Dielectric Elastomers as Electromechanical Transducers: Fundamentals, Materials, Devices, Models and Applications of an Emerging Electroactive Polymer Technology*, Elsevier, Amsterdam **2008**.

- [5] Y. Huang, G. Rui, Q. Li, E. Allahyarov, R. Li, M. Fukuto, G.-J. Zhong, J.-Z. Xu, Z.-M. Li, P. L. Taylor, L. Zhu, *Nat. Commun.* **2021**, 12, 675.
- [6] Y. Liu, H. Aziguli, B. Zhang, W. Xu, W. Lu, J. Bernholc, Q. Wang, *Nature* **2018**, 562, 96.
- [7] M. Shirvanimoghaddam, K. Shirvanimoghaddam, M. M. Abolhasani, M. Farhangi, V. Z. Barsari, H. Liu, M. Dohler, M. Naebe, *IEEE Access* **2019**, 7, 94533.
- [8] Y. Liu, H. Wang, W. Zhao, M. Zhang, H. Qin, Y. Xie, *Sensors* **2018**, 18, 645.
- [9] S.-T. Han, H. Peng, Q. Sun, S. Venkatesh, K.-S. Chung, S. C. Lau, Y. Zhou, V. A. L. Roy, *Adv. Mater.* **2017**, 29, 1700375.
- [10] F. Xu, X. Li, Y. Shi, L. Li, W. Wang, L. He, R. Liu, *Micromachines* **2018**, 9, 580.
- [11] F. Narita, M. Fox, *Adv. Eng. Mater.* **2018**, 20, 1700743.
- [12] Z. Yang, S. Zhou, J. Zu, D. Inman, *Joule* **2018**, 2, 642.
- [13] H. Maiwa, in *Piezoelectric Materials* (Ed: T. Ogawa), IntechOpen, Rijeka **2016**, Ch. 6.
- [14] C. Chen, X. Wang, Y. Wang, D. Yang, F. Yao, W. Zhang, B. Wang, G. A. Sewvandi, D. Yang, D. Hu, *Adv. Funct. Mater.* **2020**, 30, 2005141.
- [15] M. T. Chorsi, E. J. Curry, H. T. Chorsi, R. Das, J. Baroody, P. K. Purohit, H. Ilies, T. D. Nguyen, *Adv. Mater.* **2019**, 31, 1802084.
- [16] X. Tang, X. Wang, R. Cattley, F. Gu, A. D. Ball, *Sensors* **2018**, 18, 4113.
- [17] N. A. Spaldin, R. Ramesh, *Nat. Mater.* **2019**, 18, 203.
- [18] Q. Zheng, B. Shi, Z. Li, Z. L. Wang, *Adv. Sci.* **2017**, 4, 1700029.
- [19] C. Covaci, A. Gontean, *Sensors* **2020**, 20, 3512.
- [20] G. Clementi, F. Cottone, A. Di Michele, L. Gammaitoni, M. Mattarelli, G. Perna, M. López-Suárez, S. Baglio, C. Trigona, I. Neri, *Energies* **2022**, 15, 6227.
- [21] M. D. Sosa, I. K. Levy, F. Owusu, F. Nüesch, D. M. Opris, R. M. Negri, L. M. Saleh Medina, *Mater. Chem. Phys.* **2022**, 286, 126175.
- [22] I. K. Levy, F. Owusu, T. Geiger, F. Clemmens, F. Nüesch, D. M. Opris, R. M. Negri, *Eur. Polym. J.* **2022**, 180, 111616.
- [23] K. I. Park, C. K. Jeong, N. K. Kim, K. J. Lee, *Nano Convergence* **2016**, 3, 12.
- [24] H. Zhou, Y. Zhang, Y. Qiu, H. Wu, W. Qin, Y. Liao, Q. Yu, H. Cheng, *Biosens. Bioelectron.* **2020**, 168, 112569.
- [25] V. Vallem, Y. S. Sargolzaei, M. Ozturk, Y.-C. Lai, M. D. Dickey, *Adv. Mater.* **2021**, 33, 2004832.
- [26] R. Gerhard, *Proc. SPIE* **2016**, 97980T.
- [27] J. Chen, Q. Qiu, Y. Han, D. Lau, *Renewable Sustainable Energy Rev.* **2019**, 101, 14.
- [28] S. Katzir, *Arch. Hist. Exact Sci.* **2003**, 57, 61.
- [29] S. Katzir, *Stud. Hist. Philos. Sci., Part B* **2003**, 34, 579.
- [30] R. Gerhard, in *Electromechanically Active Polymers: A Concise Reference* (Ed: F. Carpi), Springer International Publishing, Cham, Switzerland **2016**, p. 489.
- [31] S. Katzir, *Stud. Hist. Philos. Sci., Part B* **2003**, 34, 579.
- [32] A. Jain, P. K. J., A. K. Sharma, A. Jain, R. P. N., *Polym. Eng. Sci.* **2015**, 55, 1589.
- [33] G. H. Haertling, *J. Am. Ceram. Soc.* **1999**, 82, 797.
- [34] Y. Xu, *Ferroelectric Materials and Their Applications*, Elsevier, Amsterdam, **1991**, p. 60.
- [35] E. K. Akdogan, M. Allahverdi, A. Safari, *IEEE Trans. Ultrason. Ferroelectr. Freq. Control* **2005**, 52, 746.
- [36] E. Fukada, *J. Phys. Soc. Jpn.* **1955**, 10, 149.
- [37] E. Fukada, I. Yasuda, *J. Phys. Soc. Jpn.* **1957**, 12, 1158.
- [38] C. A. Bassett, R. O. Becker, *Science* **1962**, 137, 1063.
- [39] M. H. Shamos, L. S. Lavine, M. I. Shamos, *Nature* **1963**, 197, 81.
- [40] E. Fukada, I. Yasuda, *J. Appl. Phys.* **1964**, 3, 117.
- [41] M. H. Shamos, L. S. Lavine, *Nature* **1967**, 213, 267.
- [42] E. Fukada, *Wood Sci. Technol.* **1968**, 2, 299.
- [43] H. Kawai, *J. Appl. Phys.* **1969**, 8, 975.
- [44] N. A. Suttle, *Mater. Des.* **1988**, 9, 318.
- [45] J. S. Harrison, Z. Ounaies, in *Encyclopedia of Smart Materials* (Ed: M. Schwartz), John Wiley and Sons, New York **2002**.
- [46] M. Smith, S. Kar-Narayan, *Int. Mater. Rev.* **2022**, 67, 65.
- [47] E. Fukada, *Ann. N. Y. Acad. Sci.* **1974**, 238, 7.
- [48] Z. Ounaies, J. A. Young, J. S. Harrison, in *Field Responsive Polymers*, Vol. 726, American Chemical Society, Washington, DC **1999**, Ch. 6, p. 88.
- [49] C. Park, Z. Ounaies, K. E. Wise, J. S. Harrison, *Polymer* **2004**, 45, 5417.
- [50] E. Fukada, *IEEE Trans. Dielectr. Electr. Insul.* **2006**, 13, 1110.
- [51] S. Bauer, R. Gerhard-Multhaupt, G. M. Sessler, *Phys. Today* **2004**, 57, 37.
- [52] S. R. Anton, K. Farinholt, A. Erturk, *J. Intell. Mater. Syst. Struct.* **2014**, 25, 1681.
- [53] E. Fukada, *IEEE Trans. Ultrason. Ferroelectr. Freq. Control* **2000**, 47, 1277.
- [54] J. S. Hundal, R. Nath, *J. Phys. D: Appl. Phys.* **1998**, 31, 482.
- [55] A. Kachroudi, S. Basrour, L. Rufer, A. Sylvestre, F. Jomni, *Smart Mater. Struct.* **2016**, 25, 105027.
- [56] G. M. Sessler, *J. Electron.* **2001**, 51–52, 137.
- [57] S. Zhang, Y. Wang, X. Yao, P. L. Floch, X. Yang, J. Liu, Z. Suo, *Nano Lett.* **2020**, 20, 4580.
- [58] M. Krause, I. Graz, S. Bauer-Gogonea, S. Bauer, B. Ploss, M. Zirkel, B. Stadlober, U. Helbig, *Ferroelectrics* **2011**, 419, 23.
- [59] C. Baur, D. J. Apo, D. Maurya, S. Priya, W. Voit, in *Polymer Composites for Energy Harvesting, Conversion, and Storage*, Vol. 1161, American Chemical Society, Washington, DC **2014**, Ch. 1, p. 1.
- [60] J.-J. Choi, B.-D. Hahn, J. Ryu, W.-H. Yoon, B.-K. Lee, D.-S. Park, *Sens. Actuators, A* **2009**, 153, 89.
- [61] K. Kim, W. Zhu, X. Qu, C. Aaronson, W. R. McCall, S. Chen, D. J. Sirbully, *ACS Nano* **2014**, 8, 9799.
- [62] R. A. Surmenev, T. Orlova, R. V. Chernozem, A. A. Ivanova, A. Bartasyte, S. Mathur, M. A. Surmeneva, *Nano Energy* **2019**, 62, 475.
- [63] Y. S. Ko, F. A. Nüesch, D. Damjanovic, D. M. Opris, *Adv. Mater.* **2017**, 29, 1603813.
- [64] Y. S. Ko, F. A. Nüesch, D. M. Opris, *J. Mater. Chem. C* **2017**, 5, 1826.
- [65] F. Owusu, F. A. Nüesch, D. M. Opris, *Adv. Funct. Mater.* **2022**, 32, 2207083.
- [66] M. Paajanen, J. Lekkala, H. Valimaki, *IEEE Trans. Dielectr. Electr. Insul.* **2001**, 8, 629.
- [67] A. Mellinger, M. Wegener, W. Wirges, R. Gerhard-Multhaupt, *Appl. Phys. Lett.* **2001**, 79, 1852.
- [68] A. Arnau, D. Soares, in *Piezoelectric Transducers and Applications* (Ed: A. A. Vives), Springer, Berlin **2008**, p. 1.
- [69] D. Damjanovic, *J. Appl. Phys.* **1997**, 82, 1788.
- [70] R. S. Dahiya, M. Valle, *Robotic Tactile Sensing: Technologies and System*, Springer, Dordrecht, Netherlands **2013**.
- [71] A. Carter, K. Popowski, K. Cheng, A. Greenbaum, F. S. Ligler, A. Moatti, *Bioelectricity* **2021**, 3, 255.
- [72] *IEEE Standard on Piezoelectricity, ANSI/IEEE Std*, Vol. 176–1987, IEEE, New York **1988**.
- [73] B. A. Capron, D. W. Hess, *IEEE Trans. Ultrason. Ferroelectr. Freq. Control* **1986**, 33, 33.
- [74] E. Defay, in *Integration of Ferroelectric and Piezoelectric Thin Films: Concepts and Applications for Microsystems* (Ed: E. Defay), ISTE, London **2011**.
- [75] A. J. Fleming, in *Piezoelectric Transducers for Vibration Control and Damping* (Eds: S. O. R. Moheimani, A. J. Fleming), Springer, London **2006**, p. 9.
- [76] S. Hu, Z. Shi, W. Zhao, L. Wang, G. Yang, *Composites, Part B* **2019**, 160, 595.
- [77] W. A. Smith, B. A. Auld, *IEEE Trans. Ultrason. Ferroelectr. Freq. Control* **1991**, 38, 40.
- [78] E. Fukada, M. Date, *J. Macromol. Sci., –Phys. B* **1973**, 8, 463.

- [79] E. Fukada, *Q. Rev. Biophys.* **1983**, 16, 59.
- [80] R. Hayakawa, Y. Wada, in *Advances in Polymer Science*, Springer, Berlin **2005**, p. 11.
- [81] L. E. Cross, in *Ferroelectric Ceramics* (Eds: N. Setter, E. L. Colla), Monte Verità, Birkhäuser, Switzerland **1993**.
- [82] T. J. Lewis, presented at *Annual Report Conf. on Electrical Insulation and Dielectric Phenomena*, Cancun, October **2002**.
- [83] S. Katzir, in *The Beginnings of Piezoelectricity: A Study in Mundane Physics* (Ed: S. Katzir), Springer, Dordrecht, the Netherlands **2006**.
- [84] D. Damjanovic, M. D. Maeder, P. D. Martin, C. Voisard, N. Setter, *J. Appl. Phys.* **2001**, 90, 5708.
- [85] R. Kressmann, *J. Appl. Phys.* **2001**, 90, 3489.
- [86] S. Bauer, *IEEE Trans. Dielectr. Electr. Insul.* **2006**, 13, 953.
- [87] R. Dahiya, M. Valle, *Robotic Tactile Sensing*, Springer, Berlin **2013**.
- [88] M. Stewart, M. G. Cain, in *Characterisation of Ferroelectric Bulk Materials and Thin Films*, Springer, Dordrecht, Netherlands **2014**, p. 37.
- [89] Y. Zhang, C. R. Bowen, S. K. Ghosh, D. Mandal, H. Khanbareh, M. Arafa, C. Wan, *Nano Energy* **2019**, 57, 118.
- [90] T. Yamada, T. Ueda, T. Kitayama, *J. Appl. Phys.* **1982**, 53, 4328.
- [91] R. Gerhard, presented at *2014 IEEE Conf. on Electrical Insulation and Dielectric Phenomena (CEIDP)*, Des Moines, October **2014**.
- [92] R. Gerhard, S. Bauer, X. Qiu, presented at *2016 IEEE Conf. on Electrical Insulation and Dielectric Phenomena (CEIDP)*, Toronto, October **2016**.
- [93] M. Habib, I. Lantgjos, K. Hornbostel, *J. Phys. D: Appl. Phys.* **2022**, 55, 423002.
- [94] J. E. Q. Quinsaat, M. Alexandru, F. A. Nüesch, H. Hofmann, A. Borgschulte, D. M. Opris, *J. Mater. Chem. A* **2015**, 3, 14675.
- [95] J. E. Q. Quinsaat, F. A. Nüesch, H. Hofmann, D. M. Opris, *RSC Adv.* **2016**, 6, 44254.
- [96] A. Sutka, P. C. Sherrell, N. A. Shepelin, L. Lapcinskis, K. Malnieks, A. V. Ellis, *Adv. Mater.* **2020**, 32, 2002979.
- [97] A. L. Skov, Q. Pei, D. Opris, R. J. Spontak, G. Gallone, H. Shea, M. Y. Benslimane, in *Electromechanically Active Polymers* (Ed: F. Carpi), Springer, Switzerland **2016**, Ch. 31, p. 687.
- [98] D. M. Opris, M. Molberg, C. Walder, Y. S. Ko, B. Fischer, F. A. Nüesch, *Adv. Funct. Mater.* **2011**, 21, 3531.
- [99] D. M. Opris, *Adv. Mater.* **2018**, 30, 1703678.
- [100] S. B. Lang, D. K. Das-Gupta, in *Handbook of Advanced Electronic and Photonic Materials and Devices* (Ed: H. Singh Nalwa), Academic Press, Burlington **2001**, p. 1.
- [101] R. E. Newnham, D. P. Skinner, L. E. Cross, *Mater. Res. Bull.* **1978**, 13, 525.
- [102] V. L. Stuber, D. B. Deutz, J. Bennett, D. Cannel, D. M. de Leeuw, S. van der Zwaag, P. Groen, *Energy Technol.* **2019**, 7, 177.
- [103] M. Yan, Z. Xiao, J. Ye, X. Yuan, Z. Li, C. Bowen, Y. Zhang, D. Zhang, *Energy Environ. Sci.* **2021**, 14, 6158.
- [104] X. Gao, M. Zheng, X. Yan, J. Fu, M. Zhu, Y. Hou, *J. Mater. Chem. C* **2019**, 7, 961.
- [105] X. Gao, M. Zheng, X. Yan, J. Fu, Y. Hou, M. Zhu, *Nanoscale* **2020**, 12, 5175.
- [106] G. Zhang, P. Zhao, X. Zhang, K. Han, T. Zhao, Y. Zhang, C. K. Jeong, S. Jiang, S. Zhang, Q. Wang, *Energy Environ. Sci.* **2018**, 11, 2046.
- [107] M.-H. Lee, A. Halliyal, R. E. Newnham, *J. Am. Ceram. Soc.* **1989**, 72, 986.
- [108] J. Feenstra, H. A. Sodano, *J. Appl. Phys.* **2008**, 103, 124108.
- [109] A. Lutsch, *Nature* **1959**, 184, 1458.
- [110] S. Qian, L. Qin, J. He, N. Zhang, J. Qian, J. Mu, W. Geng, X. Hou, X. Chou, *Mater. Lett.* **2020**, 261, 127119.
- [111] R. Tandon, D. Chaubey, R. Singh, N. Soni, *J. Mater. Sci. Lett.* **1993**, 12, 1182.
- [112] H. Banno, *Ferroelectrics* **1983**, 50, 3.
- [113] K. Ogura, M. Nishiki, H. Banno, *J. Appl. Phys.* **1992**, 31, 278.
- [114] I. Choudhry, H. R. Khalid, H.-K. Lee, *ACS Appl. Electron. Mater.* **2020**, 2, 3346.
- [115] X. Jiang, S. Wen, L. Zhang, L. Liu, *Polym.-Plast. Technol. Eng.* **2008**, 47, 1273.
- [116] C. K. Jeong, J. Lee, S. Han, J. Ryu, G.-T. Hwang, D. Y. Park, J. H. Park, S. S. Lee, M. Byun, S. H. Ko, K. J. Lee, *Adv. Mater.* **2015**, 27, 2866.
- [117] X. Chou, J. Zhu, S. Qian, X. Niu, J. Qian, X. Hou, J. Mu, W. Geng, J. Cho, J. He, C. Xue, *Nano Energy* **2018**, 53, 550.
- [118] Y. Liu, L. Zhao, L. Wang, H. Zheng, D. Li, R. Avila, K. W. C. Lai, Z. Wang, Z. Xie, Y. Zi, X. Yu, *Adv. Mater. Technol.* **2019**, 4, 1900744.
- [119] X. Huang, Q. Qin, X. Wang, H. Xiang, J. Zheng, Y. Lu, C. Lv, K. Wu, L. Yan, N. Wang, C. Xia, Z. L. Wang, *ACS Nano* **2021**, 15, 19783.
- [120] J. E. Q. Quinsaat, T. de Wild, F. A. Nüesch, D. Damjanovic, R. Krämer, G. Schürch, D. Häfliger, F. Clemens, T. Sebastian, M. Dascalu, D. M. Opris, *Composites, Part B* **2020**, 198, 108211.
- [121] X. Niu, W. Jia, S. Qian, J. Zhu, J. Zhang, X. Hou, J. Mu, W. Geng, J. Cho, J. He, X. Chou, *ACS Sustainable Chem. Eng.* **2019**, 7, 979.
- [122] W. M. Winslow, *J. Appl. Phys.* **1949**, 20, 1137.
- [123] H. A. Pohl, K. Pollock, J. S. Crane, *J. Biol. Phys.* **1978**, 6, 133.
- [124] M. A. Gutiérrez, H. Khanbareh, S. van der Zwaag, *Comput. Mater. Sci.* **2016**, 112, 139.
- [125] C. A. Randall, D. V. Miller, J. H. Adair, A. S. Bhalla, *J. Mater. Res.* **1993**, 8, 899.
- [126] S. Mamada, N. Yaguchi, M. Hansaka, M. Yamato, H. Yoshida, *J. Appl. Polym. Sci.* **2014**, 39862.
- [127] Y. Qi, N. T. Jafferis, K. Lyons, C. M. Lee, H. Ahmad, M. C. McAlpine, *Nano Lett.* **2010**, 10, 524.
- [128] Y. Qi, J. Kim, T. D. Nguyen, B. Lisko, P. K. Purohit, M. C. McAlpine, *Nano Lett.* **2011**, 11, 1331.
- [129] M. Scheffler, P. Colombo, in *Cellular Ceramics: Structure, Manufacturing, Properties and Applications* (Eds: M. Scheffler, P. Colombo), Wiley-VCH, Weinheim, Germany **2005**.
- [130] P. Colombo, *Philos. Trans. R. Soc., A* **2006**, 364, 109.
- [131] A. R. Studart, U. T. Gonzenbach, E. Tervoort, L. J. Gauckler, *J. Am. Ceram. Soc.* **2006**, 89, 1771.
- [132] K. Rittenmyer, T. Shrout, W. A. Schulze, R. E. Newnham, *Ferroelectrics* **1982**, 41, 189.
- [133] K. Hikita, K. Yamada, M. Nishioka, M. Ono, *Ferroelectrics* **1983**, 49, 265.
- [134] A. M. Varaprasad, K. Uchino, *Ferroelectr. Lett. Sect.* **1987**, 7, 89.
- [135] J. Li, Y. Yang, H. Jiang, Y. Wang, Y. Chen, S. Jiang, J.-M. Wu, G. Zhang, *Composites, Part B* **2022**, 232, 109617.
- [136] Y. Zhang, C. K. Jeong, J. Wang, H. Sun, F. Li, G. Zhang, L.-Q. Chen, S. Zhang, W. Chen, Q. Wang, *Nano Energy* **2018**, 50, 35.
- [137] Y. Zhang, C. K. Jeong, T. Yang, H. Sun, L.-Q. Chen, S. Zhang, W. Chen, Q. Wang, *J. Mater. Chem. A* **2018**, 6, 14546.
- [138] Y. S. Ko, F. Nüesch, D. M. Opris, *Poleable Dielectric Elastomer Composites*, Ecole Polytechnique Fédérale de Lausanne, Lausanne **2017**.
- [139] Z. Zhang, C. Yao, Y. Yu, Z. Hong, M. Zhi, X. Wang, *Adv. Funct. Mater.* **2016**, 26, 6760.
- [140] S.-H. Park, H. B. Lee, S. M. Yeon, J. Park, N. K. Lee, *ACS Appl. Mater. Interfaces* **2016**, 8, 24773.
- [141] Y. Duan, Y. Ding, J. Bian, Z. Xu, Z. Yin, Y. Huang, *Polymers* **2017**, 9.
- [142] M. J. Moody, C. W. Marvin, G. R. Hutchison, *J. Mater. Chem. C* **2016**, 4, 4387.
- [143] C. Li, X. Tian, T. He, *Int. J. Energy Res.* **2021**, 45, 7235.
- [144] A. Mohebbi, F. Mighri, A. Ajji, D. Rodrigue, *Adv. Polym. Technol.* **2018**, 37, 468.
- [145] F.-L. Jin, M. Zhao, M. Park, S.-J. Park, *Polymers* **2019**, 11, 953.
- [146] W. R. McCall, K. Kim, C. Heath, G. La Pierre, D. J. Sirbully, *ACS Appl. Mater. Interfaces* **2014**, 6, 19504.
- [147] M. A. Ansari, P. Somdee, *Adv. Energy Sustainable Res.* **2022**, 3, 2200063.

- [148] P. Fang, X. Qiu, W. Wirges, R. Gerhard, L. Zirkel, *IEEE Trans. Dielectr. Electr. Insul.* **2010**, 17, 1079.
- [149] P. Fang, M. Wegener, W. Wirges, R. Gerhard, L. Zirkel, *Appl. Phys. Lett.* **2007**, 90, 192908.
- [150] F. Galantini, G. Gallone, F. Carpi, *IEEE Trans. Dielectr. Electr. Insul.* **2012**, 19, 1203.
- [151] J.-J. Wang, J.-W. Tsai, Y.-C. Su, *J. Micromech. Microeng.* **2013**, 23, 075009.
- [152] S. P. Lacour, I. Graz, D. Cotton, S. Bauer, S. Wagner, presented at *2011 Annual Int. Conf. of the IEEE Engineering in Medicine and Biology Society*, August–September **2011**.
- [153] Y. Suzuki, in *Micro Energy Harvesting* (Eds: D. Briand, E. Yeatman, S. Roundy), Wiley-VCH GmbH & Co. KGaA, Weinheim, Germany **2015**.
- [154] J.-W. Tsai, J.-J. Wang, Y.-C. Su, *Sens. Actuators, A* **2014**, 215, 176.
- [155] J. Zhong, Y. Ma, Y. Song, Q. Zhong, Y. Chu, I. Karakurt, D. B. Bogy, L. Lin, *ACS Nano* **2019**, 13, 7107.
- [156] H. Hu, *Polym. Eng. Sci.* **2022**, 62, 3694.
- [157] S. W. Ma, Y. J. Fan, H. Y. Li, L. Su, Z. L. Wang, G. Zhu, *ACS Appl. Mater. Interfaces* **2018**, 10, 33105.
- [158] R. Zentel, G. Reckert, *Makromol. Chem.* **1986**, 187, 1915.
- [159] R. Zentel, *Liq. Cryst.* **1988**, 3, 531.
- [160] R. Zentel, *Angew. Chem.* **1989**, 101, 1437.
- [161] R. Zentel, G. Reckert, S. Bualek, H. Kapitza, *Makromol. Chem.* **1989**, 190, 2869.
- [162] M. Portugall, H. Ringsdorf, R. Zentel, *Makromol. Chem.* **1982**, 183, 2311.
- [163] R. Zentel, H. Ringsdorf, *Makromol. Chem., Rapid Commun.* **1984**, 5, 393.
- [164] H. Finkelmann, H.-J. Kock, G. Rehage, *Makromol. Chem., Rapid Commun.* **1981**, 2, 317.
- [165] G. H. F. Bergmann, H. Finkelmann, V. Percec, M. Zhao, *Macromol. Rapid Commun.* **1997**, 18, 353.
- [166] B. Donnio, H. Wermter, H. Finkelmann, *Macromolecules* **2000**, 33, 7724.
- [167] B. Reck, H. Ringsdorf, *Makromol. Chem., Rapid Commun.* **1985**, 6, 291.
- [168] M. Engel, B. Hisgen, R. Keller, W. Kreuder, B. Reck, H. Ringsdorf, H. W. Schmidt, P. Tschirner, *Pure Appl. Chem.* **1985**, 57, 1009.
- [169] Y. Li, T. Liu, V. Ambrogio, O. Rios, M. Xia, W. He, Z. Yang, *ACS Appl. Mater. Interfaces* **2022**, 14, 14842.
- [170] W. Meier, H. Finkelmann, *Makromol. Chem., Rapid Commun.* **1990**, 11, 599.
- [171] S. U. Vallerien, F. Kremer, E. W. Fischer, H. Kapitza, R. Zentel, H. Poths, *Makromol. Chem., Rapid Commun.* **1990**, 11, 593.
- [172] H. Hirschmann, W. Meier, H. Finkelmann, *Proc. SPIE* **1991**, 1559, 27.
- [173] P. Papadopoulos, P. Heinze, H. Finkelmann, F. Kremer, *Macromolecules* **2010**, 43, 6666.
- [174] A. Jákli, N. Éber, *Curr. Opin. Chem. Eng.* **2013**, 2, 120.
- [175] J. Seo, J. Hur, M.-S. Kim, T.-G. Lee, S. J. Seo, S. H. Han, J.-H. Seo, *Chem. Eng. J.* **2021**, 426, 130792.
- [176] R. Fu, L. Tu, Y. Guan, Z. Wang, C. Deng, P. Yu, G. Tan, C. Ning, L. Zhou, *Nano Energy* **2022**, 103, 107784.
- [177] J. Seo, B. Kim, M.-S. Kim, J.-H. Seo, *ACS Macro Lett.* **2021**, 10, 1371.
- [178] A. G. B. da Cruz, J. C. Góes, S. D. Figueiró, J. P. A. Feitosa, N. M. P. S. Ricardo, A. S. B. Sombra, *Eur. Polym. J.* **2003**, 39, 1267.
- [179] R. Liu, Q. Zhang, L. E. Cross, *J. Appl. Polym. Sci.* **1999**, 73, 2603.
- [180] M. Zhu, J. Zhang, W. Xu, R. Xiong, C. Huang, *Cellulose* **2023**, 30, 1981.
- [181] G. de Marzo, V. M. Mastronardi, L. Algieri, F. Vergari, F. Pisano, L. Fachechi, S. Marras, L. Natta, B. Spagnolo, V. Brunetti, F. Rizzi, P. Pisanello, M. De Vittorio, *Adv. Electron. Mater.* **2022**, 2200069.
- [182] J. Sun, H. Guo, J. Ribera, C. Wu, K. Tu, M. Binelli, G. Panzarasa, F. Schwarze, Z. L. Wang, I. Burgert, *ACS Nano* **2020**, 14, 14665.
- [183] X. Tian, J. Jin, S. Yuan, C. K. Chua, S. B. Tor, K. Zhou, *Adv. Energy Mater.* **2017**, 7, 1700127.
- [184] S. Tibbits, presented at *TED Conf.*, Long Beach, February, **2013**.
- [185] H. A. Alshahrani, *J. Sci.: Adv. Mater. Devices* **2021**, 6, 167.
- [186] Z. Guan, L. Wang, J. Bae, *Mater. Horiz.* **2022**, 9, 1825.
- [187] Z. Faraji Rad, P. D. Prewett, G. J. Davies, *Microsyst. Nanoeng.* **2021**, 7, 71.
- [188] A. Marino, J. Barsotti, G. de Vito, C. Filippeschi, B. Mazzolai, V. Piazza, M. Labardi, V. Mattoli, G. Ciofani, *ACS Appl. Mater. Interfaces* **2015**, 7, 25574.
- [189] C. Zhang, Y. Li, W. Kang, X. Liu, Q. Wang, *Sustainable Mater.* **2021**, 1, 127.
- [190] H. Ikram, A. Al Rashid, M. Koç, *Mod. Polym. Mater. Environ. Appl., Int. Semin., 6th* **2022**, 43, 6355.
- [191] X. Chen, H. O. T. Ware, E. Baker, W. Chu, J. Hu, C. Sun, *Procedia CIRP* **2017**, 65, 157.
- [192] E. Cesewski, A. P. Haring, Y. Tong, M. Singh, R. Thakur, S. Laheri, K. A. Read, M. D. Powell, K. J. Oestreich, B. N. Johnson, *Lab Chip* **2018**, 18, 2087.
- [193] D. McCoul, S. Rosset, S. Schlatter, H. Shea, *Smart Mater. Struct.* **2017**, 26, 125022.
- [194] J.-I. Park, G.-Y. Lee, J. Yang, C.-S. Kim, S.-H. Ahn, *J. Compos. Mater.* **2015**, 50, 1573.



Francis Owusu received his Bachelor's degree in Chemistry from Kwame Nkrumah University of Science and Technology, Ghana, and Master's degree in materials chemistry from Chalmers University of Technology, Sweden. He is currently working toward his Ph.D. degree at the Swiss Federal Laboratories for Materials Science and Technology (Empa), and enrolled in the doctoral program in chemistry and chemical engineering of the Ecole Polytechnique Fédérale de Lausanne (EPFL), Switzerland. His current research interests include piezoelectric elastomer materials, polymer synthesis and processing, nanomaterials, and polymer nanocomposites.



Thulasinath Raman Venkatesan did his Master's degree from the Joint Master of Science Program in Polymer Science of the four universities in Berlin and Potsdam. After completing his Master's degree in 2017, he pursued his joint Ph.D. in applied polymer science and physics at the University of Potsdam in Germany and KU Leuven in Belgium, respectively. Currently, he is a postdoc at Empa, Dübendorf in Switzerland, working in the Functional Polymers Laboratory.



Frank A. Nüesch graduated in physics at the Swiss Federal Institute of Technology in Zurich (ETHZ) in 1989. He earned his Ph.D. in 1995 in the field of photoinduced heterogeneous electron transfer processes in dye sensitized solar cells at the laboratory of Prof. Grätzel at the EPFL. In 2004 he was appointed Head of the Functional Polymers Laboratory at Empa where he pursued research and development of organic solar cells, organic light-emitting diodes, and electromechanical elastomer actuators. Since 2011 he is adjunct professor at EPFL teaching organic semiconductors, optical properties of materials and modern photovoltaics.



Ricardo Martin Negri is a Doctor in Chemistry from the University of Buenos Aires (UBA, 1991) and performed his postdoc at the Katholieke Universiteit Leuven (KUL, Belgium). Since 2001 he has been a professor at UBA and a scientist leader group of INQUIMAE. His research focuses on material science, particularly developing devices such as physical and chemical sensors, membranes, and electronic noses-tongues using hybrid organic-inorganic materials. He is currently working with international and local industries in R&D projects.



Dorina M. Opris studied chemistry at Babes-Bolyai University, Cluj-Napoca, Romania. Subsequently, she joined Natex S.A., developing food flavors. In 2001 she joined the group of Prof. Schlüter at Freie Universität Berlin, where she received her Ph.D. (2005). In 2006 she joined Empa, as postdoc, then as a scientist and group leader. Since 2018 she has been a lecturer at ETHZ. Her research focuses on synthesizing dielectric elastomers and exploring their potential in transducers. The European Research Council (ERC) awarded one of the prestigious ERC Consolidator for her research in 2020. Since 2023 she has been an adjunct professor at ETHZ.